Natural Resources Canada | Ressources naturelles Canada

GEOLOGICAL SURVEY OF CANADA
OPEN FILE 7875

# Geophysical surveys, permafrost conditions and infrastructure damage along the northern Yukon Alaska Highway

G.A. Oldenborger, A.-M. LeBlanc, C.W. Stevens,
J. Chartrand and B. Loranger

2015

Canada


**GEOLOGICAL SURVEY OF CANADA**
**OPEN FILE 7875**

# Geophysical surveys, permafrost conditions and infrastructure damage along the northern Yukon Alaska Highway

**G.A. Oldenborger[1], A.-M. LeBlanc[1], C.W. Stevens[2], J. Chartrand[1] and B. Loranger[3]**

[1]Geological Survey of Canada, Natural Resources Canada, Ottawa, Ontario
[2]SRK Consulting (U.S.) Inc., Anchorage, Alaska
[3]Laval University, Québec, Quebec

## 2015

© Her Majesty the Queen in Right of Canada, as represented by the Minister of Natural Resources Canada, 2015

doi:10.4095/296704

This publication is available for free download through GEOSCAN (http://geoscan.nrcan.gc.ca/).

**Recommended citation**
Oldenborger, G.A., LeBlanc, A-M., Stevens, C.W., Chartrand, J., and Loranger, B., 2015. Geophysical surveys, permafrost conditions and infrastructure damage along the northern Yukon Alaska Highway; Geological Survey of Canada, Open File 7875, 61 p. doi:10.4095/296704

Publications in this series have not been edited; they are released as submitted by the author.

## SUMMARY

The Yukon Alaska Highway is a vital transportation route connecting the resource rich Yukon to southern Canada and serving as a commercial trade and tourist route between Canada and Alaska and between the lower US and Alaska. The construction and maintenance of transportation infrastructure in permafrost regions presents challenges and costs that do not exist in other areas due to sensitivity of the engineering properties of the substrate to changes in temperature. For the Yukon Alaska Highway, road surface and embankment damage can be associated with the prevalence of warm, ice-rich permafrost. Geophysical surveys can potentially provide valuable information on permafrost and ground-ice conditions. In cooperation with Yukon Highways and Public Works, three sections of the northern Yukon Alaska Highway (23 km) have been identified for testing the usefulness of geophysical surveys for understanding permafrost degradation and assisting with highway management. Results from capacitive resistivity and ground-penetrating radar surveys were analysed and interpreted along with surficial maps, records from geotechnical borehole investigations, and surface observations of highway distress such as roughness, longitudinal cracking, embankment failures and differential settlements. Several relationships are observed. 1) Linear settlements are the most frequent and severe type of observed damage often affecting both the road surface and the embankment. 2) High degrees of road roughness tend to occur over areas mapped as till, however, identified problem areas are largely associated with fluvial and glaciofluvial map units. 3) Observed damage often occurs with high degrees of highway roughness, but high degrees of roughness are not necessarily accompanied by observable damage. 4) There is no single consistent relationship between roughness or observed damage and borehole observations of ice-rich sediment or massive ice; observed damage appears to be associated with a variety of local ground ice conditions. 5) The geophysical results help elucidate the terrain conditions and support the conclusion that multiple subsurface processes contribute to highway degradation. Several geophysical signatures are interpreted as indicative of terrain conditions involving ice-rich ground, frozen ground, thaw-susceptible sediments and shallow groundwater. Interpretation of the geophysical results is considered most reliable when done in a local context and supported by additional data such as boreholes.

## TABLE OF CONTENTS

## PREFACE

At the end of fiscal year 2013, the Geological Survey of Canada prepared a report entitled "Permafrost geophysics: Applications along the Yukon Alaska Highway" in collaboration with Yukon Highways and Public Works (Oldenborger et al., 2013). This report was submitted by Yukon Highways and Public Works (YHPW) to the Transport Canada Network of Expertise on Permafrost. The report discussed the use of geophysical techniques to map and characterize permafrost terrain. The intent was to assess the application of geophysics to infrastructure management of the Yukon Alaska Highway, and to assist YHPW in the process of contracting geophysical surveys and utilizing the results in conjunction with other available data. YHPW has since acquired a suite of geophysical data along a 190 km section of the northern Yukon Alaska Highway (Hammond, 2013). This Open File reproduces some of the material in the aforementioned Transport Canada report, but is focused on analysis and interpretation of the geophysical survey results made available by YHPW. In general, this Open File supersedes the previous Transport Canada report, although the latter contains some additional review material and discussion of the potential applicability of a larger range of geophysical methods to a variety of targets.

## INTRODUCTION

In Canada, northern highways provide vital transportations routes for communities and resource development projects. The construction and maintenance of transportation infrastructure in permafrost regions presents challenges that do not exist in other areas due to temperature sensitivity of the substrate and its engineering properties. Warm permafrost is especially challenging because it is very sensitive to any increase in heat flow from the surface. Increased heat flow can be caused by climate warming, construction activities, or the presence of infrastructure (e.g., de Grandpré et al., 2012; LeBlanc et al., 2015). In areas where transportation infrastructure crosses warm, ice-rich permafrost, the ground surface may subside rapidly causing damage to adjacent and overlying infrastructure. Distresses such as longitudinal cracking, embankment failures and differential settlements are common and maintenance costs in these areas are significantly higher than for regions without permafrost (McGregor et al., 2008).

In Yukon, approximately 25% of the highways are constructed through areas that are underlain by permafrost (Murchison, 2012). Much of the infrastructure-bearing permafrost in Yukon is warm and susceptible to degradation (Smith et al., 2010; Smith and Ednie, 2013). For the Yukon Alaska Highway, differential settlement of the embankment has led to additional annual maintenance and rehabilitation costs up to $36k/km per year – a ten-fold increase compared to non-permafrost sections of highway (Murchison, 2012). Permafrost is likely to continue to disappear from warm areas and the potential for damage is significant for regions of high ice content or massive ice. There is significant financial motivation to fully understand and mitigate the impacts of permafrost on highway infrastructure.

Permafrost distribution is discontinuous in Yukon (Hegginbottom et al., 1995; Bonnaventure et al., 2012) and its detection from the surface is difficult (or impossible post-construction) and can often only be confirmed by drilling boreholes. Boreholes can be costly and only provide point data that may not be representative of the surrounding conditions. Geophysical data can provide rapid, inexpensive and multidimensional information on permafrost conditions over extensive areas such as long transportation corridors, and are therefore valuable in the planning and maintenance of land-based infrastructure (e.g., Brown et al., 1985; Oldenborger et al., 2012). However, acquisition of quality geophysical data can be complicated and interpretation of geophysical results may be subject to significant uncertainty and non-uniqueness (e.g., Kneisel et al., 2008; Hauck, 2013).

Yukon Highways and Public Works (YHPW) has utilized geophysical surveys in an attempt to delineate subsurface conditions in permafrost regions. However, the results or interpretation of results have generally been considered unreliable or uninformative. Similar experiences are recounted in a guideline document from the Transportation Association of Canada (McGregor et al., 2010). Recently, YHPW embarked on a project utilizing multiple geophysical surveys in conjunction with geotechnical data for a 190 km section of the northern Yukon Alaska Highway from Burwash Landing to the Yukon/Alaska border (Lister, 2012; Hammond, 2013; Oldenborger et al., 2013; Stevens, 2014). YHPW is interested in using the geophysical survey results to provide nearly-continuous information on permafrost conditions and ground ice occurrence along long linear stretches of the Yukon Alaska Highway corridor in order to better understand road distress. Targets of interest include active layer thickness, embankment thickness, depth to

bedrock, occurrence and extent of ice-rich permafrost, and occurrence and extent of massive ice, including ice wedges. Geophysical-derived information would be used to direct maintenance towards highway sections most likely to be subject to damage, to better plan and budget for future maintenance and reconstruction costs, to guide engineering planning for the placement of geotechnical drilling and other investigations, and to establish a baseline for tracking the impact of climate change on the Yukon Alaska Highway.

In the context of these objectives for the Yukon Alaska Highway, this Open File addresses the application of geophysics to infrastructure projects in permafrost terrain with respect to understanding permafrost degradation and assisting with highway management. Three sections of the northern Yukon Alaska Highway (23 km) have been identified by YHPW as priority problem areas exhibiting significant road surface damage and requiring medium to high intensity restoration. Geophysical survey results provided by YHPW are analysed for these sections in conjunction with surficial geology, ground ice observations from geotechnical boreholes, road surface roughness measurements, and vehicle level observations of road surface damage such as longitudinal cracking, embankment failures and differential settlements.

## YUKON ALASKA HIGHWAY

The Yukon Alaska Highway is a vital transportation route. It connects the resource rich Yukon to southern Canada, it serves as a cross-border connection between Canada and Alaska and between the lower US and Alaska, and it is a popular tourist route. On a regional scale, the northern Yukon Alaska Highway passes through zones of sporadic to extensive discontinuous permafrost with low to medium ice content (Heginbottom, 1995). Recent probability-based models show this portion of the highway as extending across discontinuous permafrost and into the zone of continuous permafrost near Beaver Creek (Bonnaventure et al., 2012). Climate normals for 1971–2000 indicate mean annual air temperatures of −5.5ºC and −0.7ºC for Beaver Creek Station A (62º24’37’’N 140º52’03’’W, 649 masl) and Whitehorse Station A (60º42’34’’N 135º04’07’’W, 706.20 masl) respectively and climate normals for 1981–2010 indicate mean annual air temperatures of −4.9ºC and −0.1ºC for Beaver Creek Station A (62º24’37’’N 140º52’03’’W, 649 masl) and Whitehorse Station A (60º42’34’’N 135º04’07’’W, 706.20 masl) respectively (Government of Canada Historical Climate Data: http://climate.weather.gc.ca). Mean annual air temperature is increasing with winter temperatures increasing faster than summer temperatures (James et al., 2013; Government of Canada Historical Climate Data: http://climate.weather.gc.ca). As a result, the highway is currently experiencing differential settlement caused by the degradation of permafrost.

Research test sections have been established along the Yukon Alaska Highway to investigate local permafrost conditions (Lewkowicz et al., 2011; James et al., 2013) and to examine effects of engineering mitigation techniques (de Grandpré et al., 2010; 2012; Stephani et al., 2014). Although understanding of permafrost degradation is increasing, knowledge gaps remain with respect to permafrost distribution and characteristics over affected sections of the highway (Calmels, 2014). Three separate northern portions of the Yukon Alaska Highway have been identified by YHPW as priority problem areas requiring restoration due to significant road surface damage: 1) from km 1811.1–1814.0 near Koidern River, 2) from km 1837.5–1842.0 near Dry Creek, and 3) from km 1882.6–1898.1 north of Beaver Creek for a total of 22.9 km

(Figure 1). For each of these sections, permafrost conditions are interpreted based on geomorphological observations and geotechnical borehole records. Road surface damage is assessed using International Roughness Index (IRI) measurements and visually using vehicle-level photography. Finally, the geophysical survey results provided by YHPW are interpreted in the context of both the permafrost conditions and the damage assessment.

## Permafrost Conditions

Permafrost conditions were assessed along the stretch of the northern Yukon Alaska Highway from Kluane Lake at Destruction Bay to the Canada-US border (km 1684.0–1902.5) and individually for the three high-priority sections near Koidern River, Dry Creek, and north of Beaver Creek (Figure 1). The assessment was performed using a multi-scale approach to establish landscape order and site specific permafrost and ground ice information. Geomorphological interpretation was also conducted at specific sections of the highway using colour WorldView imagery and monochromatic stereopair airphotos.

From Kluane Lake to the US border, the Yukon Alaska Highway traverses 12 major surficial geological units of unknown thickness listed in Table 1 (Rampton 1979a,b,c,d). Ground ice conditions were analysed in the context of the surficial geology using the historical Alaska Highway borehole database (Lipovsky, 2009) and additional geotechnical boreholes drilled in 2011 (Lister, 2012) and 2013 (Stevens, 2014). Figure 2 shows a simplified summary of the 2011 and 2013 borehole observations. The general observed categories include road fill, unfrozen ground, partially frozen ground, frozen ground and ground ice described as per Table 2. Materials identified as road fill range in thickness from 2.1–11 m along the embankment, and consist primarily of wet to dry sand and gravel with cobbles. Frozen or partially frozen ground was encountered in 27 of the 51 boreholes. Gravimetric moisture contents for frozen samples ranged from 6% to 188%, with the highest values associated with organic silt and clay. Moisture contents for samples described as ICE were up to 421%. An unfrozen layer 0.9 m to 6.09 m thick was encountered between the road fill and underlying frozen or partially frozen ground. The unfrozen layer commonly consisted of moist to wet sediments. Moisture contents within the unfrozen layer ranged from 7.8% for sandy gravel to 120% for peat. Where present, permafrost is inferred to be warm with relatively high unfrozen water content. This inference is based on sediment temperatures measured during drilling (commonly between 0°C and −1°C), the observed presence of partially frozen ground (Figure 2), and recent permafrost temperatures measured along the highway corridor (Smith and Ednie, 2015).

Observations of ground ice type (Table 2) were recorded along with the average depth of occurrence intervals in the historical borehole database (Lipovsky, 2009). Inconsistencies in visual description between drillers and imprecise depth measurements may contribute to relatively high uncertainty for these borehole data. Furthermore, the database contains records ranging from the 1982–2003 such that borehole observations of ice content may not represent current conditions (Lister, 2012). Observation depths of ICE recorded within the borehole database as a function of surficial geology as mapped by Rampton (1979a,b,c,d) from Kluane Lake to the Canada-US border are shown in Figure 3. Eight of the twelve surficial geology units exhibit ICE: Cb, D (M), Db (>M), E, Fp, FG (M), M and O (Table 1). Surficial geology units without significant observations of ICE are: C, FG (>M), F (H) and V. The greatest depth of ICE

and the largest range in depth of ICE both occur within glaciofluvial sediments which are observed to have a high percentage of silt and clay (Stevens, 2014). The remaining surficial units exhibit ICE depths that are commonly less than 6 m below the ground surface (although this may be a function of borehole depth which tends to be greater for glaciofluvial sediments). A significant number of boreholes intercept ICE at a depth less than 4 m below the surface. It is likely that some of the ground ice observations from these boreholes occur in material below the mapped surficial deposit and ground ice may be present in other forms above the observation of ICE (Figure 4).

**Damage Assessment**

International Roughness Index (IRI) measurements were analysed as a function of surficial geology from Kluane Lake to the Canada-US border. IRI represents cumulative vertical displacement of a sprung mass relative to a vehicle axle over a given distance (Doré and Zubeck, 2009). IRI data provided by YHPW were measured over 100 m distances. Distributions of the 2010 IRI data are shown in Figure 5. Highway sections which include geogrid (a geosynthetic material used to reinforce earth materials) were removed from the analysis as they may not be representative of typical highway performance. Very poor highway conditions most frequently occur within Till drift (D), Till blanket (Db) and Organic (O) surficial units and, to a lesser extent, Morainal till (M). There is no obvious relationship between depth to ICE and poor IRI, but tills dominate the poor IRI regions regardless of ICE depth. Surficial geology units with better IRI distributions are: F (H), Fp and FG (>M). The fluvial materials exhibit some of the shallowest observations of ICE whereas the glaciofluvial materials exhibit the deepest and most variable observations of ICE (Figure 2). Note that the repair history, which is unaccounted for in this analysis, may bias the observed distribution of IRI values since repairs are sporadic and targeted, such that they are not evenly distributed among the mapped units.

In addition to IRI measurements, road surface damage was visually assessed along the three damage sections using vehicle-level photographs from 2010–2012. Observed damage was categorized in terms of thaw settlements and slope instabilities, but all of the observed damage was related to thaw settlement. Settlement was classified according to the following observed conditions: 1) local settlement occurring over a small area, 2) linear settlement occurring as elongate damage in any direction, and 3) general settlement occurring over large areas and affecting significant portions of the road surface and/or embankment. Local settlement includes damage such as sinking guardrails, isolated sinkholes and small depressions (Figure 6a). Linear settlement includes damage such as elongated depressions, cracking of the road surface or embankment and culvert failure (Figure 6b). General settlement includes large sections of differential settlement over the road and/or embankment (Figure 6c). In addition, the severity of the observed damage was classified in a purely relative sense as light, medium or severe.

Observations of surface damage are subjective and have not been normalized by distance which makes quantitative comparison difficult. However, by far, the most frequently occurring and the most severe damage was found to be in the form of linear settlement often accompanied by cracking of the highway or embankment surface (e.g., de Grandpré et al., 2012). Typically, linear settlements are elongated longitudinally with respect to the highway, but they can also be transverse or diagonal. Longitudinal settlements were prevalent regardless of the geographic

area. However, general settlements may be more severe depending on the geographic area. Both permafrost conditions and surficial damage are further discussed in conjunction with the geophysical survey results.

## GEOPHYSICAL METHODS

Geophysical methods respond to a variety of physical properties of the subsurface such as electrical conductivity, dielectric permittivity, seismic wave velocity, or density. These physical properties are (complicated) functions of a variety of subsurface conditions including material type, water content, water chemistry, ice content, and temperature among others (Scott et al., 1990; Knight and Endres, 2005). As such, no single geophysical technique will be applicable for all problems; a geophysical technique that works well for an application in one locale may not work well in another or at another time. Furthermore, different assemblages of subsurface conditions may give rise to equivalent geophysical data. Thus, significant factors in determining the success of a geophysical campaign are selection of the appropriate tool for the job and understanding the cause(s) of the observed data. A review of geophysical principles and methods with near-surface applications is given by Butler (2005) and in a permafrost context by Scott et al. (1990) and Kneisel et al. (2008).

Permafrost detection, mapping and characterization using geophysics is based on the sensitivity of physical properties to the presence of permafrost. In some cases, temperature alone may result in sufficient variability of physical properties for detection. However, for cryotic ground, it is the occurrence of ice versus water that typically results in the largest change of physical properties (e.g., King, 1977). However, given the large number of variables, it is not a simple task to unravel the exact cause of a geophysical response.

Kawasaki and Osterkamp (1984) summarize the applicability of geophysics to permafrost studies as addressing the following problems:

1. Detecting the presence or absence of permafrost.
2. Determining the lateral distribution, depth and thickness of permafrost.
3. Detecting the presence or absence of massive ground ice or ice-rich permafrost.
4. Determining extent of massive ground ice and/or ice-rich permafrost.
5. Establishing the properties and thickness of the active layer on a seasonal basis.
6. Measuring the physical and mechanical properties of permafrost or ground ice.
7. Miscellaneous environmental and engineering problems such as locating groundwater in permafrost terrain, detecting thawed zones, selecting pipeline or highway routes, etc.

Similar applications are described by Scott et al. (1990) and Kneisel et al. (2008) perhaps with the notable additions of long-term monitoring applications (e.g., Hilbich et al., 2008). Furthermore, in modern application, geophysical data are often used to construct a physical property model via inversion (Oldenburg and Li, 2005; Hauck 2013). These models are most often non-unique and of necessarily limited resolution. Given a physical property model recovered via inversion, it is typically by proxy or interpretation that a geological or cryostratigraphic model of the subsurface is constructed. Thus, there is potential uncertainty on several fronts: 1) errors or noise associated with the geophysical data, 2) errors associated with

the geophysical model, and 3) errors associated with interpretation or understanding. Quantitatively addressing uncertainty in geophysical results is termed the appraisal problem and it is a subject of much research on its own (e.g., Oldenburg and Li, 1999; Friedel, 2003; Day-Lewis et al., 2005; Hilbich et al., 2009; Oldenborger and Routh 2009; Oldenborger, 2014; Deceuster et al., 2014).

In planning the geophysical surveys for the Yukon Alaska Highway, the targets identified by YHPW define a general objective of detailed 2D/3D mapping of permafrost conditions and ground ice with lesser focus on characterization of permafrost properties. The ability to execute long linear surveys from the highway surface was considered paramount. As such, YHPW focussed on 2D survey methods that could be deployed from a moving vehicular platform with automated (GPS) positioning and without significant specialized setup. The chosen geophysical survey types were capacitive resistivity (CR) and ground-penetrating radar (GPR) for which commercial towed systems are available and mature. Although towed systems allow for rapid acquisition of on-road data, special consideration must be given to issues of increased noise, reliance on GPS, and sheer volume of data to be processed and analysed.

## Capacitive Resistivity

In a capacitive resistivity (CR) survey, electrical current is generated in the ground via coupling of an audio frequency alternating current across a transmitter-earth capacitor (Kuras et al., 2006; Groom, 2008). Similarly, voltage is measured via coupling of the resulting potential field across an earth-receiver capacitor. CR data are conventionally considered analogous to those from a galvanic resistivity (GR) survey, but certain conditions and corrections are applicable (e.g., Oldenborger and LeBlanc, 2013). Unlike GR surveys where electrodes are physically inserted into the ground, CR surveys are non-contacting and allow for acquisition of data where use of galvanic electrodes is prohibitive, such as along roads, or where contact resistance with the ground is extremely high such as for ice or dry soils.

The primary physical parameter governing the low-frequency electrical response is the electrical resistivity (the inverse of electrical conductivity) and a model of subsurface electrical resistivity is the typical result of a modern CR survey. In most near-surface geologic environments, controlling factors on the bulk electrical resistivity of rocks and sediments are the amount of pore fluid, the connectivity of the pore fluid, and the availability and mobility of charge-carrying ions. Permafrost can have a strong influence on electrical resistivity because low temperatures reduce the mobility of charge-carrying ions, and the freezing of water greatly reduces the availability and connectivity of pore fluid for electrolytic conduction. Consequently, resistivity is observed to increase gradually down to the freezing point and increase dramatically for temperatures below freezing (King et al., 1988; Krautblatter et al., 2010; Overduin et al., 2012). At low ground temperatures, the unfrozen water content may be reduced to a point where there is little contrast in resistivity between frozen sediment or massive ice or even air (Hoekstra et al., 1975). Nevertheless, cryotic sediments with high salinity may contain appreciable unfrozen water content due to exclusion of salts and freezing point depression (Grimm et al., 2008). Similarly, cryotic fine-grain soil may contain appreciable unfrozen water content due to tension forces, to the point where permafrost may be quite conductive for certain material types (e.g., King, 1977; Ross et al., 2007; Oldenborger et al., 2015).

In permafrost terrain, measurements of electrical resistivity can generally be used to infer some combination of the pore-fluid conductivity and the moisture content, or similarly, the material type and the amount of frozen/unfrozen water. As such, electrical and electromagnetic geophysics can be applied in an attempt to map material type and to characterize occurrence of ice-bearing permafrost, thaw zones and thermophysical transitions underground.

## Ground-Penetrating Radar

Ground-penetrating radar (GPR) or georadar involves the propagation of high frequency electromagnetic waves (Annan, 2005). GPR is considered separately from electromagnetic methods because when operated according to basic design principles, it responds primarily to variations in the dielectric permittivity (or radar wave speed) of the subsurface and electrical conductivity affects only the attenuation or radar range. Permafrost terrain is a good candidate for GPR surveys due to the typically low electrical conductivity (high resistivity) of ground ice which yields good penetration, and due to the significant difference between the dielectric constants (and radar wave speed) for water and ice.

GPR is historically rooted in permafrost applications (Annan and Davis 1976; Moorman et al., 2003). GPR differs from electrical and electromagnetic methods in that it is a wave-based method yielding high-resolution results that are often readily interpretable without significant processing. Active layer characteristics and location of taliks or massive ground ice are traditional GPR targets (Scott et al., 1990; Arcone et al., 1998) in addition to locating ice wedges (Fortier and Allard 2004) and mapping stratigraphy (Stevens et al., 2009). Very high water content, the presence of saline pore water, or significant clay fraction can render GPR inapplicable. Most recently, GPR has seen increased use in multi-method investigations, usually coupled with electrical methods, to provide some cryostratigraphic constraint on the subsurface thereby reducing uncertainty in the interpretation (De Pascale et al., 2008; Fortier et al., 2011; Angelopoulos et al., 2013). Fortier and Savard (2010) present a case study at Tasiujaq Airport where GPR is used to define the cryostratigraphic contacts while CR is used to characterize permafrost conditions such as unfrozen ground and taliks. These interpretations are then related to observed sections of thaw settlement on the runway and the thaw-sensitive stratigraphy is identified.

## Other Geophysical Methods

Although not utilized in this study of the Yukon Alaska Highway, other geophysical methods may be applicable for infrastructure permafrost investigations. As with CR, GR responds to the electrical conductivity of the ground and may provide more detailed information than CR when ground contact is possible (Oldenborger and LeBlanc, 2013). Electromagnetic methods respond to the complex electrical conductivity and are applicable to similar situations as GR and CR surveys, with certain operational benefits and drawbacks (Hoekstra et al., 1975; Todd and Dallimore, 1998; Fitterman and Labson, 2005; Zonge et al., 2005).

In general, seismic methods respond to variations in seismic wave speed which is a function of the density and elastic parameters of the material (Pelton, 2005). Compressional and shear wave

velocities increase sharply for ice-bearing permafrost due to a reduction in the unfrozen water content (King et al., 1988). This increase is more significant for higher-porosity materials for which a larger portion of the material can transition from a liquid to solid phase. It is interesting to note that seismic methods respond primarily to the solid phase whereas electrical and electromagnetic methods respond primarily to the liquid phase; this can result in complimentary sensitivities, particularly during freeze or thaw (Hauck et al., 2011).

Seismic data acquisition is broadly generalized into reflection and refraction methods. Reflection methods provide some indication of stratigraphy and of thermal horizons such as top or bottom of permafrost, but are typically applied for deep exploration targets. Reflection methods (especially shear wave methods) have not been as widely applied to near-surface permafrost investigations as refraction methods due to the difficulty in collecting high-quality, high-resolution data at shallow depths (e.g., Skvortsov et al., 1992; Steeples and Miller, 1998). Refraction methods provide information on the seismic wave speed distribution of the subsurface and can be used to measure depth to frozen ground or variations in thaw depth (Huasmann et al., 2007). Tomographic analysis can provide more detailed images of the seismic wave speed distribution in permafrost (Maurer and Hauck, 2007). Refraction generally requires that seismic wave speed increases with depth and results are complicated by the limited contrast in velocity between ice and bedrock and the occurrence of low velocity layers. Some of these issues can be mitigated with transmission-type experiments (e.g., LeBlanc et al., 2004).

Other geophysical methods that have seen less widespread application to permafrost investigations are gravity surveys (Kawasaki et al., 1982; Scott et al., 1990; Hausmann et al., 2007), magnetometric resistivity surveys (Edwards and Nabighian, 1991), nuclear magnetic resonance surveys (Kleinberg and Griffin, 2005; Parsekian et al., 2013), radiometric borehole logging (Scott et al., 1990), magnetotellurics and controlled-source audio magnetotellurics (Scott et al., 1990). Gravity surveys require great care in obtaining data of good enough quality to detect density anomalies associated with ice, especially when the density of ice can be variable (Annan and Davis, 1990). Magnetometric resistivity (MMR) surveys are overshadowed by the familiarity with and proliferation of advanced processing software for electrical resistivity data, but there is likely some benefit in the enhanced signal penetration. Nuclear magnetic resonance (NMR) is a relatively young method, although commercial equipment is available and it shows great promise in that it responds directly to unfrozen water content. Radiometric methods require handling of active gamma and neutron radiation sources and are limited to borehole data. Magnetotellurics (MT) and controlled-source audio magnetotellurics (CSAMT) are applicable when deep exploration may be required, but otherwise, near-surface resolution is limited.

## RESULTS

The CR and GPR geophysical surveys along the Yukon Alaska Highway were conducted simultaneously in October 2012 by Golder Associates Ltd. (Hammond, 2013). Data were collected from km 1709.5–1902.5 (Figure 1) along a single linear profile using a Geometrics OhmMapper and a MALÅ ProEX. Data collection was performed in two separate passes along the highway shoulder with different acquisition parameters.

CR data were collected with 5 m and 10 m antenna lengths giving depths of investigation of approximately 2–5 m and 4–11 m respectively. Data were de-spiked, smoothed, grouped in 5 km sections and inverted to recover 2D models of electrical resistivity (Hammond, 2013). Data were inverted assuming straight-line geometry and artefacts may be present for sections of road with significant curvature over the length of the antenna array. CR survey results (as provided by YHPW) were delivered as electrical resistivity sections in 3 km increments with severe vertical exaggeration. The delivered resistivity models were interpolated to a uniform grid for display using a linear color scale. Results were provided with identification of high and low resistivity zones, with some interpretation examples and with observations from the 2011 geotechnical boreholes (Lister, 2011). Many of the increments exhibit gridding effects such as striping. In addition, the recovered resistivity values do not necessarily span the range of the associated color scale. Neither the raw data, nor the un-interpolated models recovered via inversion, nor the inversion parameters and convergence behaviour were available for analysis.

GPR data were collected with 250 MHz and 100 MHz shielded antennas. GPR data were processed with zero-time adjustment, average trace removal, variable gain and high-pass filtering (Hammond, 2013). GPR survey results (as provided by YHPW) were delivered as interpreted significant coherent reflections in 3 km increments. These reflection surfaces result from structural, textural, or moisture related changes of the subsurface materials. For the sections considered here, there are few interpreted coherent reflections below the reflection identified as the base of road fill. As such, only the base of road fill reflection is presented. Neither the raw data, nor the GPR reflection amplitudes are available for analysis of features such as radar facies, reflection character, ringing or noise. However, some instances of GPR signal attenuation are noted (Hammond, 2013).

Geophysical survey results provided by YHPW are reproduced here for each of the identified priority damage sections in Figures 7–32 in the delivered 3 km increments with observations from the 2011 geotechnical boreholes (Lister, 2011). Electrical resistivity and GPR reflections are combined with ground ice observations from the historical Alaska Highway borehole database (Lipovsky, 2009), surficial geology according to the Yukon terrain classification system (Lipovsky and Bond, 2014) and WorldView-2 satellite images from 27 August 2010 (copyright DigitalGlobe Inc., all rights reserved). Each 3 km increment is analyzed in conjunction with IRI measurements provided by YHPW and vehicle-level road surface damage observations from 2010, 2011 and 2012. Results are presented only for increments of the damage sections along which road surface damage was actually observed. Geotechnical information from the historical Alaska Highway borehole database is used to construct logs of primary sediment texture and ground ice information to assist in interpretation of the geophysical results.

## 1. Koidern River

The Koidern River highway section extends from km 1811.1–1814.0 (Figure 1) and crosses a fluvial plain consisting of silt with an organic surface cover (Figures 7–9). The fluvial plain extends to the southeast and is occupied by the Koidern River in this location. Further to the northwest of the damage section, the highway crosses two fluvial terraces as observed from airphotos. Geotechnical boreholes indicate that the sediment texture transitions from mostly silt with sand to sand and gravel across the adjacent fluvial terraces. The highway section extends

across thermokarst terrain which closely follows the limit of the silt-rich fluvial plain and is absent across the coarser-grained fluvial terraces. Boreholes confirm that ground ice (ICE, Vs and Vr) is a major component of the cryostratigraphy (Figure 10). Ground ice may have formed via in-situ ice segregation within the silty sediments which are spatially limited and may delimit a palsa plateau (Calmels et al., 2015).

Highway damage along the Koidern River section was identified in 2010 mostly as light-to-severe linear settlement coincident with very poor IRI measurements (Figure 7). After repairs in the summer of 2011, IRI measurements remained poor, but observable surficial damage was largely mitigated (Figure 8 and 9). Of interest to note is that observable surface damage is usually coincident with poor (2.5–3.5 m/km) to very poor (3.5–10 m/km) IRI measurements. Conversely, poor and very poor IRI measurements are not necessarily accompanied by observable surface damage as classified here using vehicle-level photographs. Observable damage appears to be confined to the thermokarst terrain and coincident with observations of ground ice, whereas poor to very poor IRI measurements extend across thermokarst terrain into morainal tills with no observed ground ice.

Despite the multiple borehole observations of ground ice, recovered electrical resistivity is generally low along the Koidern River section. The transition from the more resistive morainal tills (300–800 Ωm) to silt-rich ground (<400 Ωm) is apparent near 1809.9 km. Below the interpreted depth of road fill, a conductive anomaly extends from 1810–1812 km which corresponds to the extent of thermokarst terrain and may result from appreciable unfrozen water in the silty sediments (Figure 10). Observed damage does not seem to be related to the conductive anomaly over its entire length. In fact, the 2010 observed damage and the historical ground ice observations occur within a region of increased resistivity (1811.1–1811.6 km). This zone of increased resistivity is interpreted to represent ice-rich frozen ground that is undergoing degradation in the midst of relatively unfrozen and wet, but more stable ground. After repairs in 2010, the IRI measurements over the interpreted frozen ground continued to increase whereas the remaining IRI values, although poor, remained the same.

The increase in resistivity at approximately 8 m depth at 1810.3 km may represent the frozen sediment observed in borehole BH11-29 in 2011. However, resolution loss at depth and model smoothness make identification of a transition at depth difficult; the conductive anomaly at the bottom of BH11-29 is very likely an artefact (Figure 7). The increase in resistivity at approximately 7 m depth at the eastern end of the section is interpreted as the bedrock signature. Also due to resolution loss, the magnitude of the recovered resistivity is not likely representative of the true resistivity, but a bedrock interpretation is consistent with surficial mapping of weathered bedrock along the section.

**2. Dry Creek**

The Dry Creek section extends from km 1837.5–1842.0 (Figure 1) and crosses glaciofluvial and organic terrain underlain by McConnell age glaciofluvial sediments (Figures 11–13). The primary sedimentary textures are gravel and sand (Figure 14). There is evidence of thermokarst north of the highway right-of-way (Calmels et al., 2015), but no evidence of ice wedges is observed from airphoto interpretation along the Dry Creek section.

The average depth of ICE recorded in the historical borehole database ranges from 7.3–11.3 m below the surface, which is deeper than for the Koidern River section. The ICE is often overlain by Vx ground ice (Figure 14). The general cryostratigraphy for the glaciofluvial deposit is characterized by relatively ice-poor sands and gravels underlain by deep-seated ground ice below about 6–7 m. Given the low potential for ice segregation in sand and gravel, it is postulated that the ground ice described in the geotechnical boreholes for the Dry Creek section represents relic massive ice buried under glaciofluvial deposits. Alternatively, ice-rich permafrost may have formed prior to deposition of the glaciofluvial deposit within an unknown underlying unit.

Highway damage was identified at 15 specific sites in 2010 (Figure 11). Observed damage includes all forms of settlement characterized mostly as moderate to severe. The Dry Creek section has the highest occurrence of severe damage for the sections studied herein, mostly in the form of general settlement. Local and linear settlements predominately occur on the west side of the highway, extending from the embankment to the adjacent highway lanes. Again, observed damage coincides with poor and very poor IRI measurements, but there are many poor and very poor IRI measurements that have no apparent associated damage. After repairs in the summers of 2010 and 2011, much of the observed damage was mitigated (Figure 12). IRI measurements decreased in repaired areas, but not to the point of being considered good or even ok. In 2012, IRI measurements are observed to have increased and observable damage is again apparent, indicating continued degradation (Figure 13).

Observed road damage near 1840.6 and 1841.4 km is associated largely with unfrozen sand and gravel (glaciofluvial) with limited potential for segregation ice (Figures 11 and 14). However, there is a distinct cluster of ICE and other ground-ice observations located west of the road (Figure 15) and, to a lesser extent, east of the road (Figure 11). There is apparent correspondence between ice occurrence, observed damage and poor IRI measurements near 1840.6 km. The absence of observed thermokarst directly adjacent to the road suggests that the degradation of deep ice may be the controlling factor for this damage zone.

Borehole observations of ICE are deep, perhaps deeper than the reliable depth of investigation of the CR survey. However, there is a clear resistive anomaly (>4000 Ωm) at 1840.5 km starting around 8 m depth underneath the already resistive sands and gravels (2000–4000 Ωm). This is likely the signature of massive ice, but it does not appear to be encountered by BH11-35 (Figure 13). A similar deep resistive anomaly near 1839.7 km should also be considered as massive ice, although with significantly lesser extent. This anomaly may be associated with the damage observed near 1839.9 km in 2012 (Figure 13). In contrast, there are no observations of ICE along the road near the damage location of 1841.4 km. This damage zone is associated with a conductive anomaly (<400 Ωm) that coincides with borehole observation of unfrozen clay (Figure 14). The anomaly appears to continue into the highway embankment (Figure 11). Such an observation would be consistent with increased moisture content or active groundwater within the embankment and natural ground. Heat advection, thaw settlement of any frozen clay, mechanical erosion and seasonal freeze/thaw would all contribute to damage of the highway surface.

## 3. North of Beaver Creek

Highway damage was initially identified on vehicle-level photographs over 15.5 km from km 1882.6–1898.1 north of Beaver Creek (Figure 1). Almost all observed damage was in the form of linear differential settlement parallel or diagonal to the highway alignment. Damage is characterized mostly as light to moderate, and linear settlements are sometimes accompanied by cracking. Herein, only two 3 km increments are analysed for the section north of Beaver Creek, although all increments are presented in order from south to north in Figures 16–32.

Part 1 of the Beaver Creek section extends from km 1883–1886 over organic surficial material underlain by fluvial sediments (Figures 16–18). Thermokarst features appear across portions of the organic units. Sediment type is variable; observations of ground ice are prevalent and confined largely to silt (Figure 19). There are some observations of thick frozen organic material that will be highly susceptible to thaw settlement. This section of highway is oriented perpendicular to the direction of surface hydrological flow. Poorly-drained terrain surrounds the highway from 1884–1886 km and surface hydrology or shallow groundwater may play an important role in highway performance. Severe damage identified at 1886.1 km was attributed to culvert failure and Grandpré et al. (2010; 2012) describe a nearby site where groundwater flow is occurring across and underneath the highway embankment.

This increment of the Beaver Creek section appears to have a strong relationship between observed damage, poor IRI measurements, and the occurrence of ground ice (Figures 16 and 19). After repairs in the summer of 2011, surface damage was mitigated, but was beginning to reappear by 2012 (Figure 18). There is no obvious consistent electrical resistivity anomaly that coincides with the zones of damage. However, both sections of elevated IRI measurements exhibit reduced resistivity of the embankment material and high attenuation of the GPR signal is observed near BH11-45 (Hammond, 2013) consistent with increased unfrozen water content. These conductive embankment sections occur over silt and organics with ground ice as observed in BH11-44 and BH11-45 (Figure 16). In contrast, the highest observed embankment conductivity is from 1884.1–1884.8 km, but is over borehole observations of bedrock and gravel and coincides with stable good IRI measurements. The resistivity signature of bedrock is not readily apparent, but is interpreted as the moderately resistive anomaly (1200 Ωm) from 1884.7–1885.1 km below 1–2 m depth. The weakly resistive anomaly (800 Ωm) from 1884.2-1884.6 km below 2 m depth is interpreted as predominantly gravel (Figure 19). Therefore, it is inferred that the combination of a conductive embankment over conductive (frozen) silts represents a resistivity anomaly indicative of shallow groundwater-related settlement. However, a conductive embankment signature alone is not necessarily indicative of settlement.

Part 4 of the Beaver Creek section extends from km 1892–1895 over colluvial, alluvial and morainal till units (Figures 26–28). Sediment type under the highway is largely silt with some occurrence of sand and gravel (Figure 29). Observations of frozen material are common, but ground ice is less prevalent. In 2010, observed damage along this highway section was minimal and IRI measurements were a mixture of poor and ok stretches (Figure 26). In the summer of 2011, damage up to 1893.1 km was repaired, but the rest of this highway section exhibited significant increases in IRI measurements and the development of new surface damage (Figures 27 and 28). There is no apparent correspondence between the IRI measurements and the

observed surface damage, nor does the observed surface damage appear to correspond to observations of ground ice, although most of the highway section is on historically frozen ground (Figure 29).

The development of surface damage in 2011 and 2012 appears to coincide with a large conductive anomaly (<400 Ωm) extending from the embankment to depth along a stretch of highway oriented perpendicular to hydrologic flow from 1892.7–1893.7 km (Figures 27 and 28). Again, this conductive anomaly is interpreted as indicative of shallow groundwater over frozen (but not ice-rich and maybe warm and wet) silty material resulting in groundwater-related settlement. However, along this increment of the Beaver Creek section, from 1893.7-1895 km the conductive-over-resistive anomaly coincides with very poor IRI measurements. This is in contrast to part 1 of the Beaver Creek Section for which this same anomaly pattern coincides with good highway conditions (Figure 18). In this case, the resistive anomaly (1000–3000 Ωm) below 3 m depth from 1894–1895 km is interpreted as colder ice-rich silty sediments that are vulnerable to thaw settlement (Figure 28; Smith and Ednie, 2015). For part 1, the underlying resistive anomaly is interpreted as bedrock.

## DISCUSSION

The permafrost conditions assessed for the Koidern River, Dry Creek and Beaver Creek sections of the Yukon Alaska Highway exhibit different ground ice conditions, hydrology and surficial geology. These three study sections have been identified by YHPW as medium and high intensity restoration areas exhibiting significant damage, yet they pass over terrain types that do not have characteristically bad IRI measures of highway roughness (Figure 5). Furthermore, observed damage often occurs with high degrees of roughness, but high degrees of roughness are not necessarily accompanied by observable damage. These observations indicate that surficial geology alone is not a reliable indicator of the propensity for damage of the road surface, and that multiple processes may be responsible for highway degradation.

The geophysical surveys contracted by YHPW were conducted with the objective of characterizing permafrost conditions and mapping ice-rich ground and/or massive ice which would lead to identification of thaw sensitive areas. Analysis of the geophysical results in the context of highway roughness and observed damage allows an assessment of the usefulness of the geophysical surveys for highway management. Several different subsurface resistivity structures are observed and interpreted to represent a variety of conditions that are consistent with damage observations and support the conclusion that multiple subsurface processes contribute to highway degradation in addition to ice-rich ground or massive ice. However, no obvious electrical resistivity anomalies are observed that could be used as consistent indicators of potential degradation. Furthermore, the relationship between electrical resistivity and observed damage, or electrical resistivity and IRI measurements is complicated and site-specific.

The task of geophysical interpretation or terrain characterization is further hindered by the non-uniqueness and limited dynamic range of the CR survey results. For this survey, the range of electrical resistivity recovered via inversion is considerably less than expected for unfrozen sedimentary material, frozen ground, ice and bedrock (e.g., Palacky, 1988; Scott et al., 1990) and considerably less than that observed in other studies in the region (Lewkowicz et al., 2011). This

limited range is exacerbated by a constant linear color scale for display which should be replaced by a logarithmically-scaled and truncated color scale.

Stevens (2014) performed a comparison of hand-picked CR-derived electrical resistivity values, lithology, and cryotic state for 20 selected geotechnical boreholes from 2011 and 2013 (Figure 33). It is apparent that for the given survey, there is significant overlap in modelled electrical resistivity. For example, although frozen ground is typically more resistive than partially frozen ground, partially frozen ground is very similar in resistivity to unfrozen ground. Although silt, sand and gravel exhibit a general trend of increasing resistivity, the majority of silt and sand observations fall within the 25$^{th}$ and 75$^{th}$ percentiles of gravel observations, and the gravel observations fall within the range of frozen ground observations. In any case, clear distinction of material type or cryotic state from CR-derived electrical resistivity alone is difficult. It is expected that results could be improved by correcting the raw CR data for effective dipole length (Oldenborger and LeBlanc, 2013) or by using galvanic methods for comparison. However, a large degree of non-uniqueness is inherent to the physical principles of electrical geophysical methods. Geophysical interpretation needs to be performed in the context of local conditions (several km), relative relationships and supporting data. To help identify potential inversion artefacts and to avoid over-interpretation, some sort of uncertainty analysis would also prove beneficial.

## CONCLUSIONS

Results from CR and GPR surveys along the northern Yukon Alaska Highway were analysed and interpreted along with surficial maps, geotechnical borehole records, and surface observations of highway roughness and distress.

- Surficial damage appears to be associated with poor IRI measurements, but poor IRI measurements are not necessarily associated with observed damage. A more systematic approach is required to establish or refute any meaningful correlation between observed surficial damage (location and type) and IRI measurements.

- For highway infrastructure, the embankment plays an important role in terms of the geophysical response and the interpretation. For the Yukon Alaska Highway, GPR proved useful for estimating embankment depth; results are in good agreement with borehole observations. Identified coherent GPR reflections were largely confined to the embankment and did not provide useful information on ground ice conditions, although signal attenuation patterns were used for interpreting shallow groundwater.

- The CR geophysical results help elucidate the terrain conditions and support the conclusion that multiple subsurface processes contribute to highway degradation. Several electrical resistivity signatures are interpreted as indicative of terrain conditions involving ice-rich ground, frozen ground, thaw-susceptible sediments and shallow groundwater. However, the CR survey along the Yukon Alaska Highway exhibits limited dynamic range in modelled resistivities and consistent identification of material type or ground ice conditions is difficult. No unique resistivity signature is indicative of thaw susceptibility and no single relationship exists between CR survey results and observed damage or IRI

measurements. The geophysical results are most useful when interpreted in the context of local conditions and supporting data to yield information on permafrost, moisture content, shallow groundwater and lithology. Identification of massive ice was only possible at one site along the considered sections, and this interpretation would not be possible from CR results alone perhaps due to the warm, wet nature of the permafrost. For specifically targeting ice conditions, surveys conducted in late winter may be more effective due to increased freezing which reduces complexity in interpretation of geophysical models.

- Bedrock contact is mostly reported for boreholes north of Beaver Creek at depths less than 15 m where the highway rises onto bedrock-controlled terrain. In the case that bedrock is shallow enough, it is resolvable by CR survey results, but reliable interpretation is only possible in conjunction with supporting data due to the relatively weak resistive signature.

- The level of analysis contained herein is preliminary. Increased understanding would result from additional work on a number of fronts including advanced processing of the CR data, investigation of any statistically significant correlation between observed damage, IRI and geophysical signature, or investigation of the data in the context of climatic trends and temporal evolution of the borehole database records.

## ACKNOWLEDGEMENTS

This work was conducted under the Land-Based Infrastructure Project of the Climate Change Geoscience Program, Earth Sciences Sector, Natural Resources Canada. Yukon Highways and Public Works (P. Murchison and M. Idrees) provided highway km post data, IRI measurements, vehicle-level photography, monochromatic stereopair airphotos for specific highway sections, report 1114760059-003-R-Rev0 from Golder Associates, report 12-1348-0013 from Golder Associates, report 1CG023.001 from SRK Consulting and funding for damage assessment. The historical Alaska Highway borehole database was obtained from the Yukon Permafrost Network. The Yukon digital surficial geology compilation was obtained from the Yukon Geological Survey. Landsat 7 mosaic and shaded relief images were obtained from Yukon Geomatics. Topographic data (CanVec v11, 1:50 000 scale) were obtained from Natural Resources Canada Geogratis. National Road Network data were obtained from the Government of Canada Open Government portal. Worldview-2 satellite images, 27 August 2010, copyright DigitalGlobe Inc., all rights reserved. M. Ednie provided valuable comments and critical review.

Yukon Permafrost Network: http://permafrost.gov.yk.ca/data/arcgis
Yukon Geological Survey: http://www.geology.gov.yk.ca/digital_surficial_data.html
Yukon Geomatics: http://www.geomaticsyukon.ca/data
Natural Resources Canada Geogratis: http://geogratis.cgdi.gc.ca/
Government of Canada Open Government portal: http://open.canada.ca

## REFERENCES

Angelopoulos M.C., Pollard W.H. and Couture N.J., 2013. The application of CCR and GPR to characterize ground ice conditions at Parsons Lake, Northwest Territories. Cold Regions Science and Technology 85, 22–33.

Annan A.P., 2005. Ground-penetrating radar. In: Near-Surface Geophysics, Butler D.K., ed., 357–438. Society of Exploration Geophysicists.

Annan A.P. and Davis J.L., 1976. Impulse radar sounding in permafrost. Radio Science 11, 383–394.

Arcone S.A., Lawson D.E., Delaney A.J., Strasser J.C. and Strasser J.D., 1998. Ground-penetrating radar reflection profiling of groundwater and bedrock in an area of discontinuous permafrost. Geophysics 63, 1573–1584.

Bonnaventure P.P., Lewkowicz A.G., Kremer M. and Sawada M.C., 2012. A permafrost probability model for the southern Yukon and Northern British Columbia, Canada. Permafrost and Periglacial Processes 23, 52–68.

Brown J., Metz M.C. and Hoekstra P., 1985. Workshop on permafrost geophysics. U.S. Army Cold Regions Research and Engineering Laboratory, Special Report 85-5.

Butler D.K., ed., 2005. Near-Surface Geophysics. Society of Exploration Geophysicists.

Calmels F., 2014. Vulnerability of the north Alaska Highway to climate change, Yukon, Canada. ArcticNet Annual Scientific Meeting, Arctic Change 2014, Ottawa, ON.

Calmels F., Roy L.-P., Laurent C., Pelletier M., Kinnear L., Benkert B. and Horton B., 2015. Vulnerability of the North Alaska Highway to permafrost thaw: A field guide and data synthesis. Northern Climate ExChange, Yukon Research Centre, Yukon College.

Day-Lewis F.D., Singha K. and Binley A.M., 2005. Applying petrophysical models to radar travel time and electrical resistivity tomograms: Resolution dependent limitations. Journal of Geophysical Research 110, B08206.

de Grandpré I., Fortier D. and Stephani E., 2010. Impact of groundwater flow on permafrost degradation: Implications for transportation infrastructures. Proceedings of the Sixth Canadian Conference on Permafrost, 534–540.

de Grandpré I., Fortier D. and Stephani E., 2012. Degradation of permafrost beneath a road embankment enhanced by heat advected in groundwater. Canadian Journal of Earth Sciences 49, 953–962.

De Pascale G.P., Pollard W.H. and Williams K.K., 2008. Geophysical mapping of ground ice using a combination of capacitive coupled resistivity and ground-penetrating radar, Northwest Territories, Canada. Journal of Geophysical Research 113, F02S90.

Deceuster J., Etienne A., Robert T., Nguyen F. and Kaufmann O., 2014. A modified DOI-based method to statistically estimate the depth of investigation of dc resistivity surveys. Journal of Applied Geophysics 103, 172–185.

Doré G. and Zubeck H.K., 2009. Cold Regions Pavement Engineering. ASCE Press.

Edwards R.N. and Nabighian M.N., 1991. The magnetometric resistivity method. In: Electromagnetic Methods in Applied Geophysics, vol. 2, Nabighian M.N., ed., 47–104. Society of Exploration Geophysicists.

Fitterman D.V. and Labson V.F., 2005. Electromagnetic induction methods for environmental problems. In: Near-Surface Geophysics, Butler D.K., ed., 301–355. Society of Exploration Geophysicists.

Fortier D. and Allard M., 2004. Late Holocene syngenetic ice-wedge polygons development, Byot Island, Canadian Arctic Archipelago. Canadian Journal of Earth Sciences 41, 997–1012.

Fortier R., LeBlanc A.-M. and Yu W., 2011. Impacts of permafrost degradation on a road embankment at Umiujaq in Nunavik (Quebec), Canada. Canadian Geotechnical Journal 48, 720–740.

Fortier R. and Savard C., 2010. Engineering geophysical investigation of permafrost conditions underneath airfield embankments in Northern Quebec (Canada). Proceedings of the Sixth Canadian Conference on Permafrost, 1307–1316.

Friedel S., 2003. Resolution, stability and efficiency of resistivity tomography estimated from a generalized inverse approach. Geophysical Journal International 153, 305–316.

Groom D., 2008. Common misconceptions about capacitively-coupled resistivity (CCR): What it is and how it works. Symposium on the Application of Geophysics to Environmental and Engineering Problems, 1345–1350.

Hammond M., 2013. Shakwak Highway Project: North Alaska Highway geophysical data acquisition processing and interpretation. Golder Associates Ltd., report 12-1348-0013.

Hauck C., 2013. New Concepts in Geophysical Surveying and Data Interpretation for Permafrost Terrain. Permafrost and Periglacial Processes 24, 131–137.

Hauck C., Bottcher M. and Maurer H., 2011. A new model for estimating subsurface ice content based on combined electrical and seismic data sets. The Cryosphere 5, 453–468.

Hausmann H., Krainer K., Brückl E. and Mostler W., 2007. Internal structure and ice content of Reichenkar Rock Glacier (Stubai Alps, Austria) assessed by geophysical investigations. Permafrost and Periglacial Processes 18, 351–367.

Heginbottom J.A., Dubreuil M.H. and Harker P.T., 1995. Canada, Permafrost. National Atlas of Canada, Plate 2.1, MCR 4177.

Hilbich C., Hauck C., Scherler L., Volksch I., Vonder Muhll D. and Mausbacher R., 2008. Monitoring mountain permafrost evolution using electrical resistivity tomography: A 7-year study of seasonal, annual, and long-term variations at Schilthorn, Swiss Alps. Journal of Geophysical Research 113, F01S90.

Hilbich C., Marescot L., Hauck C. and Mausbacher R., 2009. Applicability of Electrical Resistivity Tomography Monitoring to Coarse Blocky and Ice-rich Permafrost Landforms. Permafrost and Periglacial Processes 20, 269–284.

Hoekstra P., Sellmann P.V. and Delaney A., 1975. Ground and airborne resistivity surveys of permafrost near Fairbanks, Alaska. Geophysics 40, 641–656.

James M., Lewkowicz A.G., Smith S.L. and Miceli C.M., 2013. Multi-decadal degradation and persistence of permafrost in the Alaska Highway corridor, northwest Canada. Environmental Research Letters 8, 045013.

Kawasaki K. and Osterkamp T.E., 1984. Electromagnetic induction measurements in permafrost terrain for detecting ground ice and ice-rich soils. Alaska Department of Transportation and Public Facilities, Report No. FHWA-AK-RD-85-12.

Kawasaki K., Osterkamp T.E. and Kienle J., 1982. Gravity measurements in permafrost terrain containing massive ground ice. Alaska Department of Transportation and Public Facilities, Report No. FHWA-AK-RD-83-07.

King M.S., 1977. Acoustic velocities and electrical properties of frozen sandstones and shales. Canadian Journal of Earth Sciences 14, 1004–1013.

King M.S., Zimmerman R.W. and Corwin R.F., 1988. Seismic and electrical properties of unconsolidated permafrost. Geophysical Prospecting 36, 349–364.

Kleinberg R.L. and Griffin D.D., 2005. NMR measurements of permafrost: unfrozen water assay, pore-scale distribution of ice, and hydraulic permeability of sediments. Cold Regions Science and Technology 42, 63–77.

Kneisel C., Hauck C., Fortier R. and Moorman B., 2008. Advances in geophysical methods for permafrost investigations. Permafrost and Periglacial Processes 19, 157–178.

Knight R.J. and Endres A.L., 2005. An introduction to rock physics principles for near-surface geophysics. In: Near-Surface Geophysics, Butler D.K., ed., 31–70. Society of Exploration Geophysicists.

Krautblatter M., Verleysdonk S., Flores-Orozco A. and Kemna A., 2010. Temperature-calibrated imaging of seasonal changes in permafrost rock walls by quantitative electrical resistivity tomography (Zugspitze, German/Austrian Alps). Journal of Geophysical Research 115, F02003.

Kuras O., Beamish D., Meldrum P.I. and Ogilvy R.D., 2006. Fundamentals of the capacitive resistivity technique. Geophysics 71, G135–G152.

LeBlanc A.-M., Fortier R., Allard M., Cosma C. and Buteau S., 2004. Seismic cone penetration test and seismic tomography in permafrost. Canadian Geotechnical Journal 41, 796–813.

LeBlanc A.-M., Oldenborger G.A., Sladen W.E. and Allard M., 2015. Infrastructure and climate warming impacts on ground thermal regime, Iqaluit International Airport, Nunavut. Canada-Nunavut Geoscience Office, Summary of Activities 2014, 119–132.

Lewkowicz A.G., Etzelmüller B. and Smith S.L., 2011. Characteristics of discontinuous permafrost based on ground temperature measurements and electrical resistivity tomography, southern Yukon, Canada. Permafrost and Periglacial Processes 22, 320–342.

Lipovsky P.S., 2009. Interim release of Alaska Highway borehole database. Yukon Geological Survey.

Lipovsky P.S. and Bond J.D., 2014. Yukon digital surficial geology compilation, digital release 1, 08-Apr-2014. Yukon Geological Survey.

Lister D., 2012. Geotechnical site investigation: Shakwak Highway Project–North Alaska Highway–Yukon km 1710 to km 1902. Golder Associates Ltd., report 1114760059-003-R-Rev0.

Maurer H. and Hauck C., 2007. Geophysical imaging of alpine rock glaciers. Journal of Glaciology 53, 110–120.

McGregor R.V., Hassan M. and Hayley D., 2008. Climate change impacts and adaptation: Case studies of roads in Northern Canada. Proceedings of the 2008 Annual Conference of the Transportation Association of Canada.

McGregor R., Hayley D., Wilkins G., Hoeve E., Grozic E., Roujanski V., Jansen A. and Doré G., 2010. Guidelines for development and management of transportation infrastructure in permafrost regimes. Transportation Association of Canada.

Moorman B.J., Robinson S.D. and Burgess M.M., 2003. Imaging periglacial conditions with ground-penetrating radar. Permafrost and Periglacial Processes 14, 319–329.

Murchison P., 2012. A bumpy road: Highways and thawing permafrost. MacBride Lecture, MacBride Museum of Yukon History.

Oldenborger G.A., 2014. Comment on "The application of CCR and GPR to characterize ice conditions at Parsons Lake, Northwest Territories" by Angelopoulos et al. Cold Regions Science and Technology 100, 68–70.

Oldenborger G.A. and LeBlanc A.-M., 2013. Capacitive resistivity inversion using effective dipole lengths for line antennas. Journal of Applied Geophysics 98, 229–236.

Oldenborger G.A., LeBlanc A-M. and Sladen W.E., 2015. Electrical and electromagnetic data for permafrost characterization at Iqaluit International Airport, Nunavut. Geological Survey of Canada, Open File 7750.

Oldenborger G.A. and Routh P.S., 2009. The point-spread function measure of resolution for the 3-D electrical resistivity experiment. Geophysical Journal International 176, 405–414.

Oldenborger G.A., Stevens C.W., LeBlanc A.-M., Loranger B. and Murchison P., 2013. Permafrost geophysics: Applications along the Yukon Alaska Highway. Client Report to Transport Canada Network of Expertise on Permafrost.

Oldenborger G.A., Stevens C.W. and Wolfe S.A., 2012. Electrical geophysics for assessing permafrost conditions along highway infrastructure. Proceedings of the Symposium on the Application of Geophysics to Environmental and Engineering Problems.

Oldenburg D. and Li Y., 1999. Estimating depth of investigation in dc resistivity and IP surveys. Geophysics 64, 403–416.

Oldenburg D.W. and Li Y., 2005. Inversion for applied geophysics: A tutorial. In: Near-Surface Geophysics, Butler D.K., ed., 89–150. Society of Exploration Geophysicists.

Overduin P.P., Westermann S., Yoshikawa K., Haberlau T., Romonovsky V. and Wetterich S., 2012. Geoelectric observations of the degradation of nearshore submarine permafrost at Barrow (Alaskan Beaufort Sea). Journal of Geophysical Research 117, F02004.

Palacky G.J., 1988. Resistivity characteristics of geologic targets. In: Electromagnetic Methods in Applied Geophysics, vol. 1, Nabighian M.N., ed., 53–129. Society of Exploration Geophysicists.

Parsekian A.D., Grosse G., Walbrecker J.Q., Müller-Petke M., Keating K., Liu L., Jones B.M. and Knight R., 2013. Detecting unfrozen sediments below thermokarst lakes with surface nuclear magnetic resonance. Geophysical Research Letters 40, 535–540.

Pelton J.R., 2005. Near-surface seismology: Surface-based methods. In: Near-Surface Geophysics, Butler D.K., ed., 219–263. Society of Exploration Geophysicists.

Pihlainen J.A. and Johnston G.H., 1963. Guide to a field description of permafrost; National Research Council, Technical Memorandum 79.

Rampton V.N., 1979a. Surficial geology and geomorphology, Koidern Mountain, Yukon Territory. Geological Survey of Canada, Map 5-1978.

Rampton V.N., 1979b. Surficial Geology and Geomorphology, Burwash Creek, Yukon Territory. Geological Survey of Canada, Preliminary Map 6-1978.

Rampton V.N., 1979c. Surficial Geology and Geomorphology, Generc River, Yukon Territory. Geological Survey of Canada, Preliminary Map 7-1978.

Rampton V.N., 1979d. Surficial Geology and Geomorphology, Congdon Creek, Yukon Territory. Geological Survey of Canada, Preliminary Map 8-1978.

Scott W.J., Sellmann P.V. and Hunter J.A., 1990. Geophysics in the study of permafrost. In: Geotechnical and Environmental Geophysics, Ward S.H., ed., 355–384. Society of Exploration Geophysicists.

Skvortsov A., Hunter J., Goriainov N., Burns R., Tsarov A. and Pullan S., 1992. High-resolution shear-wave reflection technique for permafrost engineering applications: New results from Siberia. SEG Expanded Abstracts, 382–384.

Smith S.L. and Ednie M., 2013. Preliminary ground thermal data from field sites established summer 2013 along the Alaska Highway easement, Yukon. Geological Survey of Canada, Open File 7507.

Smith S.L. and Ednie M., 2015. Ground thermal data collection along the Alaska Highway easement (KP 1559-1895) Yukon, summer 2014. Geological Survey of Canada, Open File 7762.

Smith S.L., Romanovsky V.E., Lewkowicz A.G., Burn C.R., Allard M., Clow G.D., Yoshikawa K. and Throop J., 2010. Thermal state of permafrost in North America: A contribution to the international polar year. Permafrost and Periglacial Processes 21, 117–135.

Steeples D.W. and Miller R.D., 1998. Avoiding pitfalls in shallow seismic reflection surveys. Geophysics 63, 1213–1224.

Stephani E., Fortier D., Shur Y., Fortier R. and Doré G., 2014. A geosystems approach to permafrost investigations for engineering applications, an example from a road stabilization experiment, Beaver Creek, Yukon, Canada. Cold Regions Science and Technology 100, 20–35.

Stevens C.W., Moorman B.J., Solomon S.M. and Hugenholtz C.H., 2009. Mapping subsurface conditions within the near-shore zone of an Arctic delta using ground penetrating radar. Cold Regions Science and Technology 56, 30–38.

Stevens C., 2014. Northern Alaska Highway geophysical validation. SRK Consulting (Canada) Inc., report 1CG023.001.

Todd B.J. and Dallimore S.R., 1998. Electromagnetic and geological transect across permafrost terrain, Mackenzie River delta, Canada. Geophysics 63, 1914–1924.

Zonge K., Wynn J. and Urquhart S., 2005. Resistivity, induced polarization and complex resistivity. In: Near-Surface Geophysics, Butler D.K., ed., 265–300. Society of Exploration Geophysicists.

## TABLES

**Table 1.** Surficial geology (Rampton 1979a,b,c,d). Reported texture of the surficial geology should be considered to be of relatively high uncertainty.

| Unit Label | Surficial Geology | Texture |
|---|---|---|
| C | Colluvium | Angular rock fragments |
| Cb | Colluvium, blanket (>1 m thick) | Mixed angular fragments, sand, silt |
| D (M) | Till, drift, McConnell age | Clay, silt, sand |
| Db (>M) | Till, blanket (>1m thick), pre-McConnell age | Sand, silt |
| E | Eolian | Sand, silt |
| F(H) | Fluvial, Holocene | Gravel |
| Fp | Fluvial plain | Silt, sand, clay to gravel, sand, silt |
| FG (M) | Glaciofluvial, McConnell age | Gravel |
| FG (>M) | Glaciofluvial, pre-McConnell age | Gravel, sand |
| M | Moraine, till | Sand, silt |
| O | Organic | Organic |
| V | Volcanic veneer (0.1–1 m thick) | Volcanic ash |

**Table 2.** Classification and description of ground ice (Pihlainen and Johnston, 1963).

| Ice Type | Description | Example Ice Structure |
|---|---|---|
| X | Not frozen | NA |
| F | Frozen: ice type unknown | NA |
| N | Nonvisible ice | NA |
| Vx | Visible ice: individual ice crystals | Ice crystals |
| Vc | Visible ice: ice coating on particles | Pore ice |
| Vr | Visible ice: random or irregular orientation | Reticulate ground ice |
| Vs | Visible ice: stratified or distinct orientation | Segregation ice |
| ICE | Visible ice: ice greater than 25 mm thick | Ice lenses |

## FIGURES

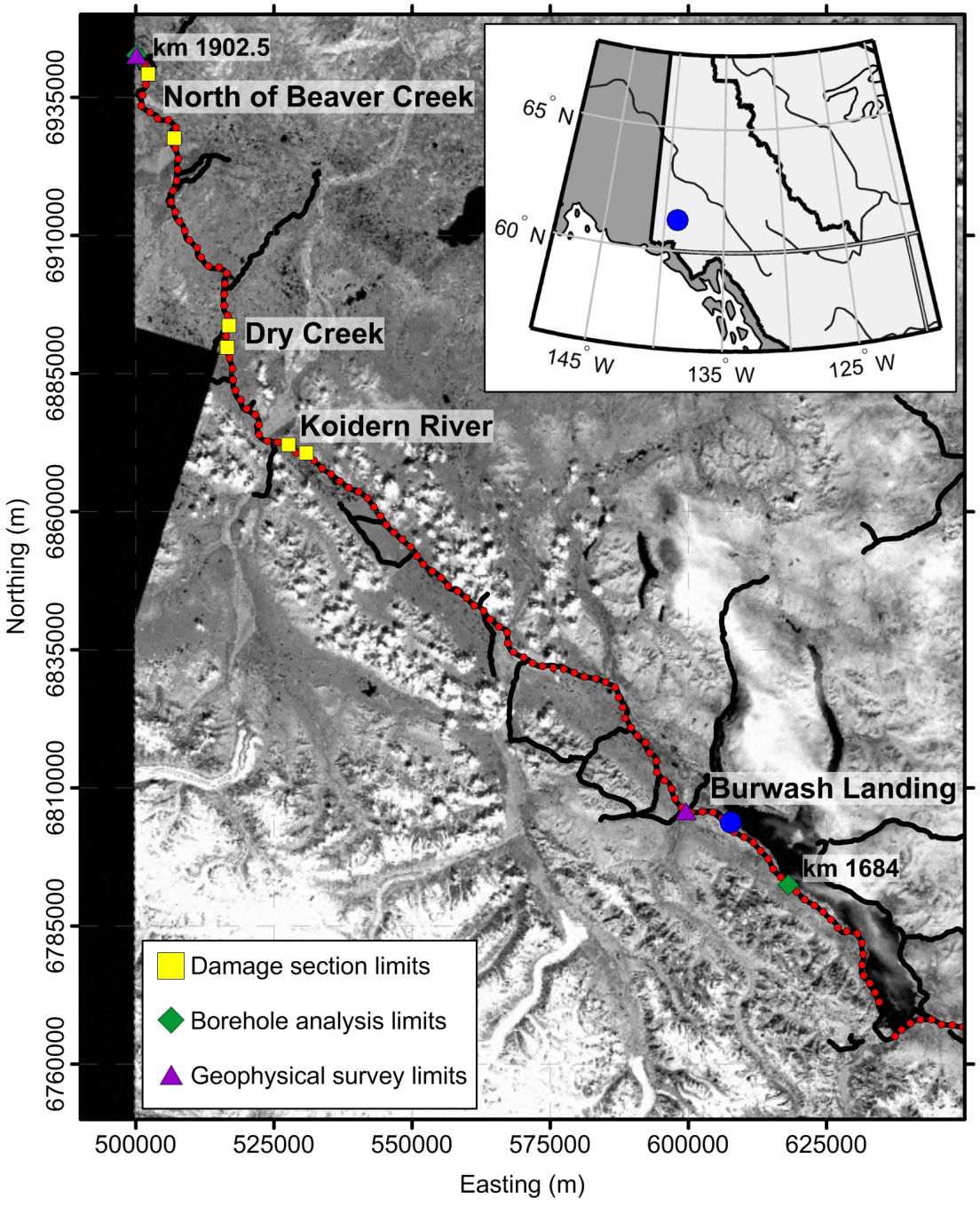


**Figure 1.** Northern Yukon Alaska Highway showing limits of the three damage sections, the geophysical surveys (km 1709.5–1902.5), and the borehole permafrost analysis (km 1684.0–1902.5).

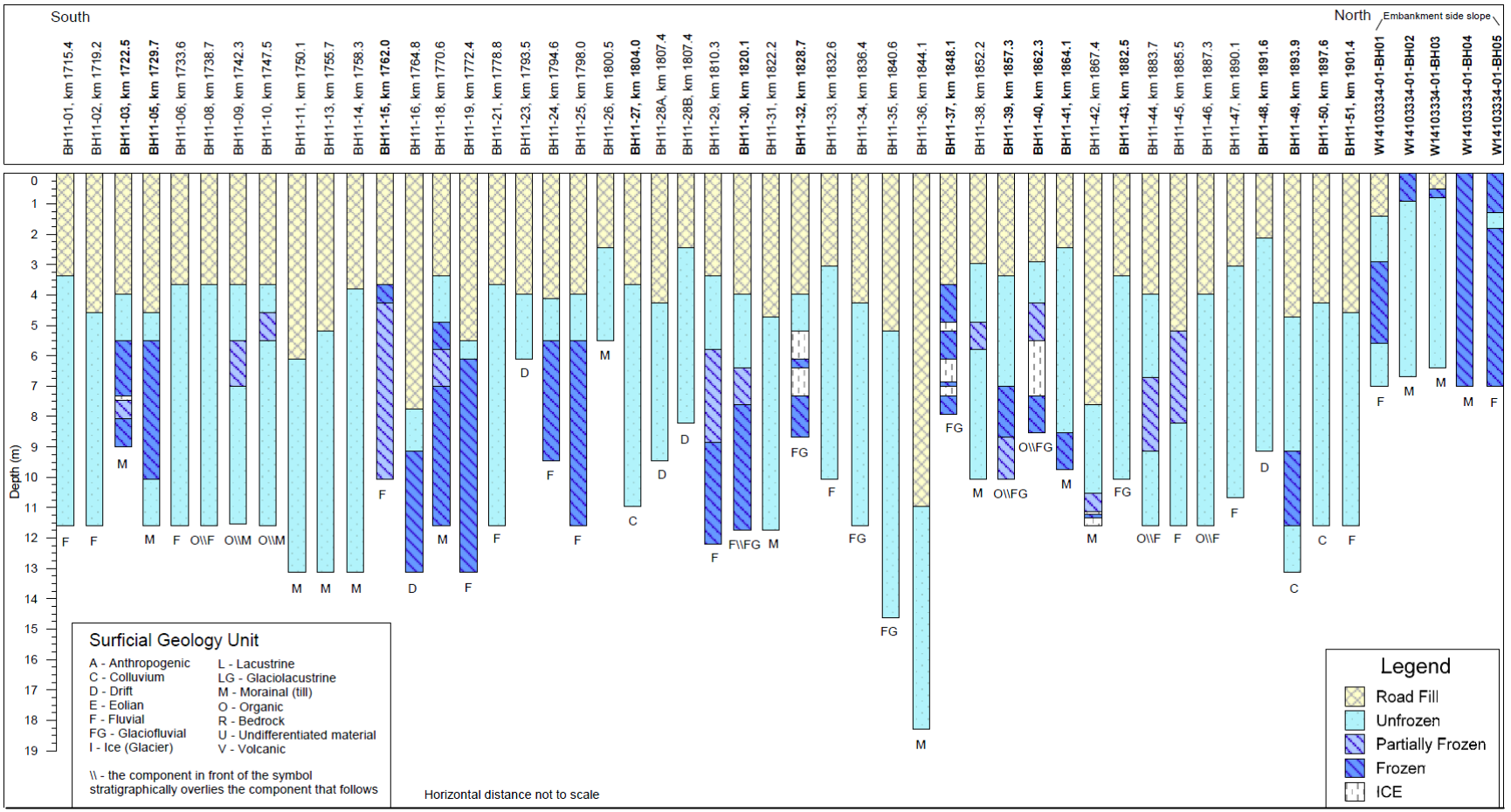


**Figure 2.** Summary of 2011 and 2013 geotechnical borehole observations along the northern Yukon Alaska Highway (Stevens, 2014). Surficial geology from (Rampton 1979a,b,c,d).

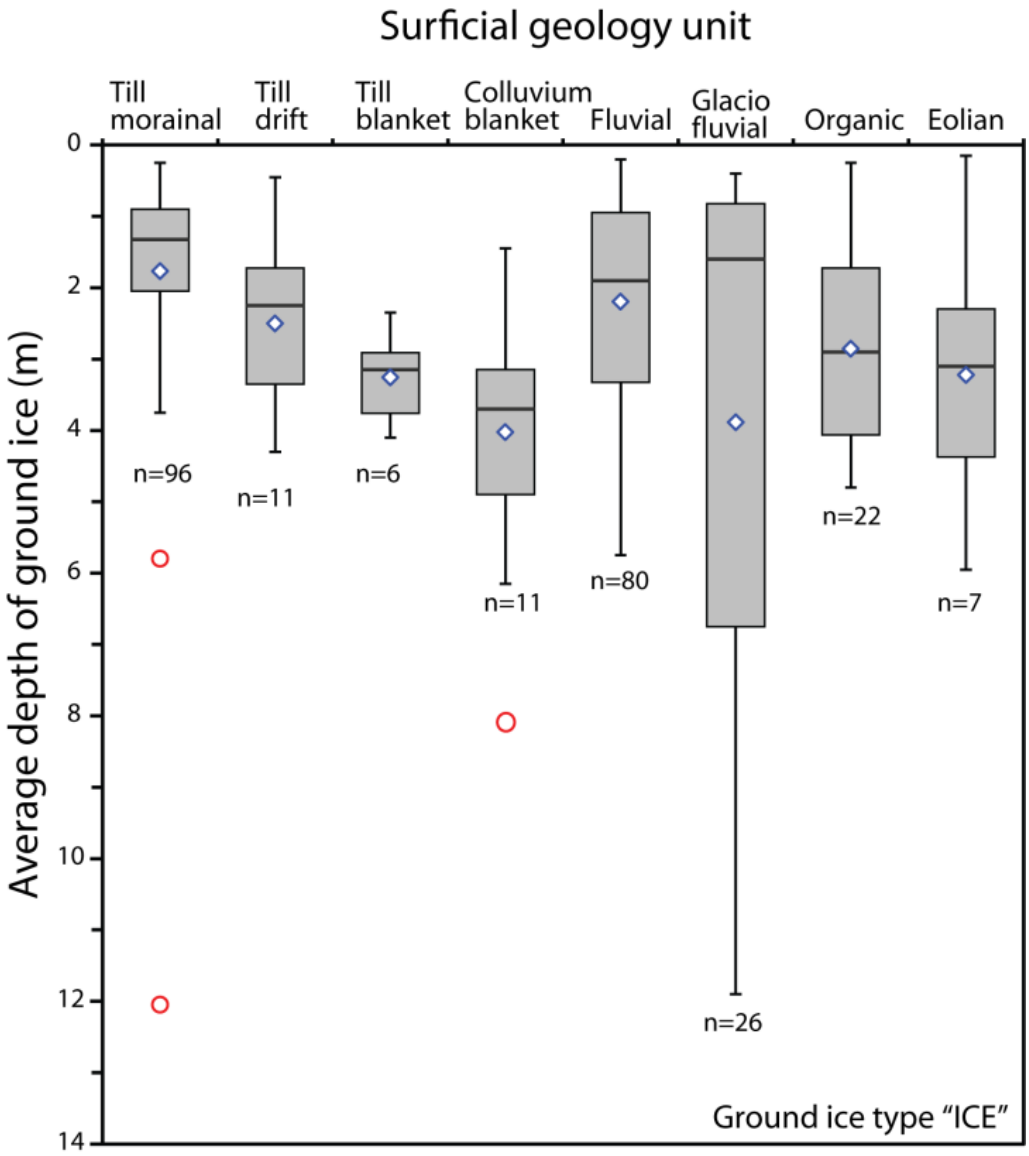


**Figure 3.** Depth of ICE for surficial geology units along the northern Yukon Alaska Highway (km 1684.0–1902.5). Mean values are represented by blue diamonds, outliers are represented by red circles, and population size *n* is given for each geological unit. Surficial geology from Rampton (1979a,b,c,d) and ground ice data from Lipovsky (2009).

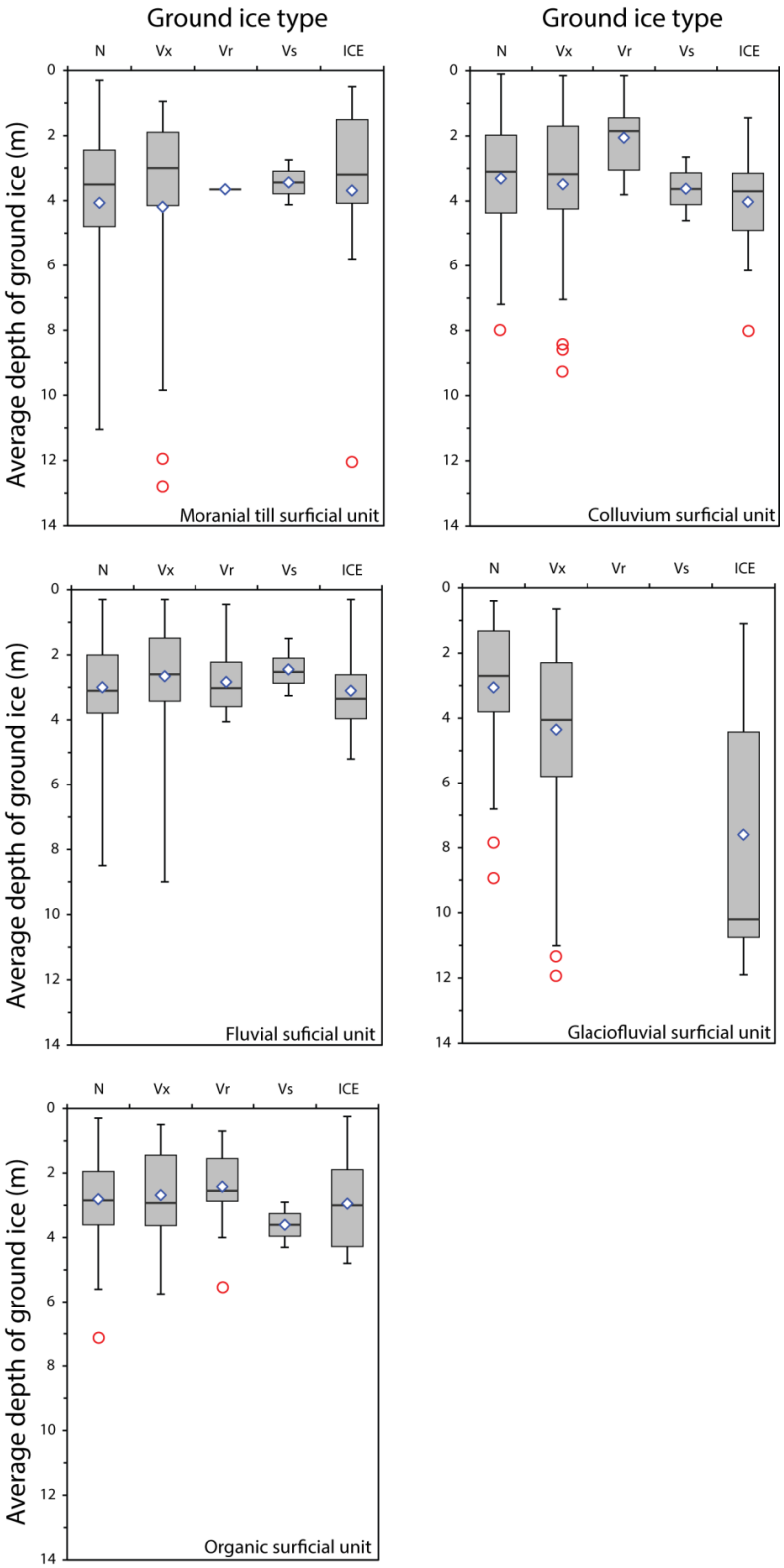


**Figure 4.** Depth of ice by ice type for surficial geology units along the northern Yukon Alaska Highway (km 1811.1–1814.0, Koidern River section). Mean values are represented by blue diamonds and outliers are represented by red circles. Surficial geology from Rampton (1979a,b,c,d) and ground ice data from Lipovsky (2009).

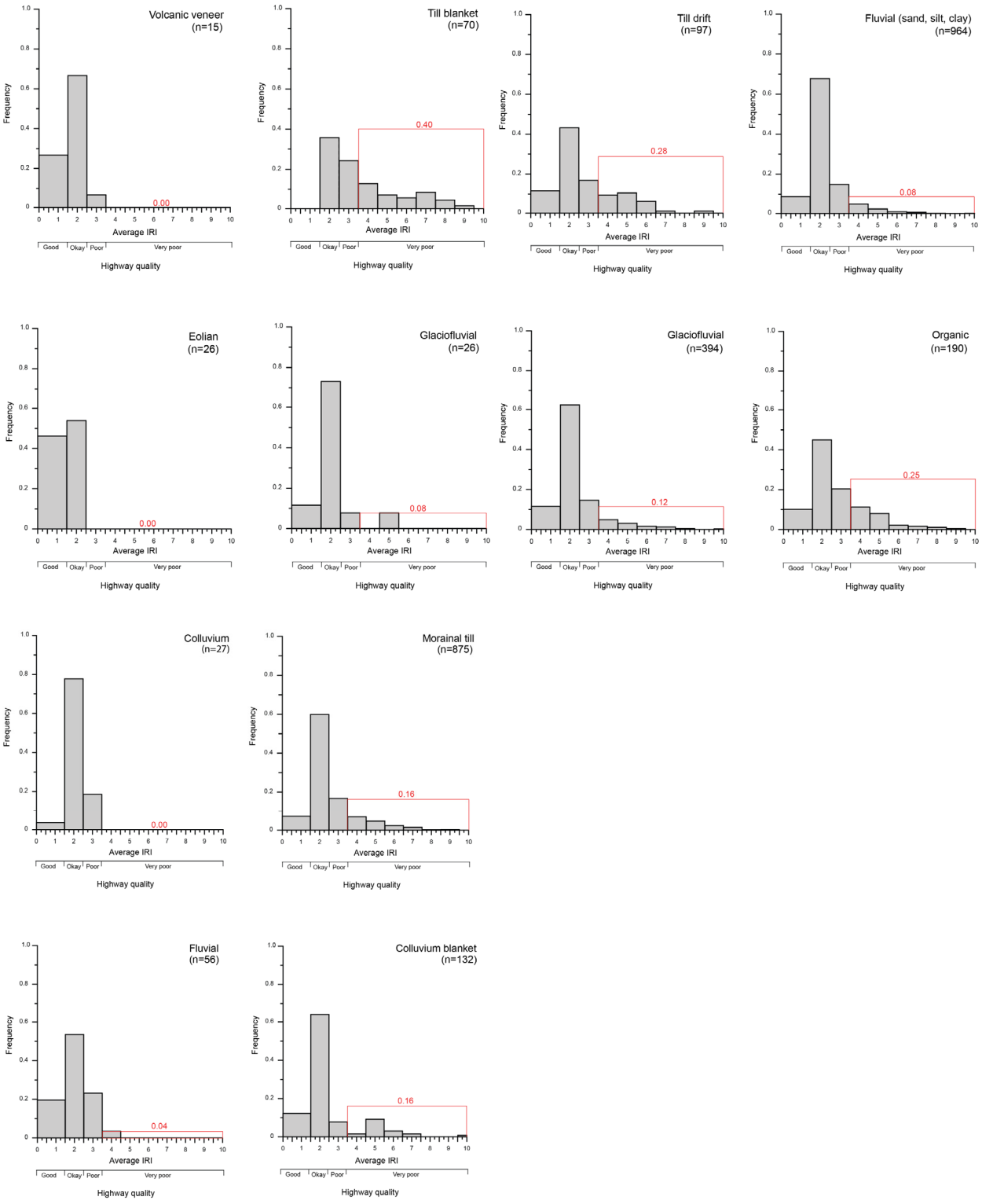


**Figure 5.** Distributions of 2010 IRI measurements for surficial geology units from km 1684.0–1902.5 along the northern Yukon Alaska Highway. IRI measurements are classified as good: 0.0–1.5 m/km, ok: 1.5–25 m/km, poor: 2.5–3.5 m/km and very poor: 3.5–10 m/km. The relative frequency of very poor conditions is indicated in red. Surficial geology from Rampton (1979a,b,c,d).

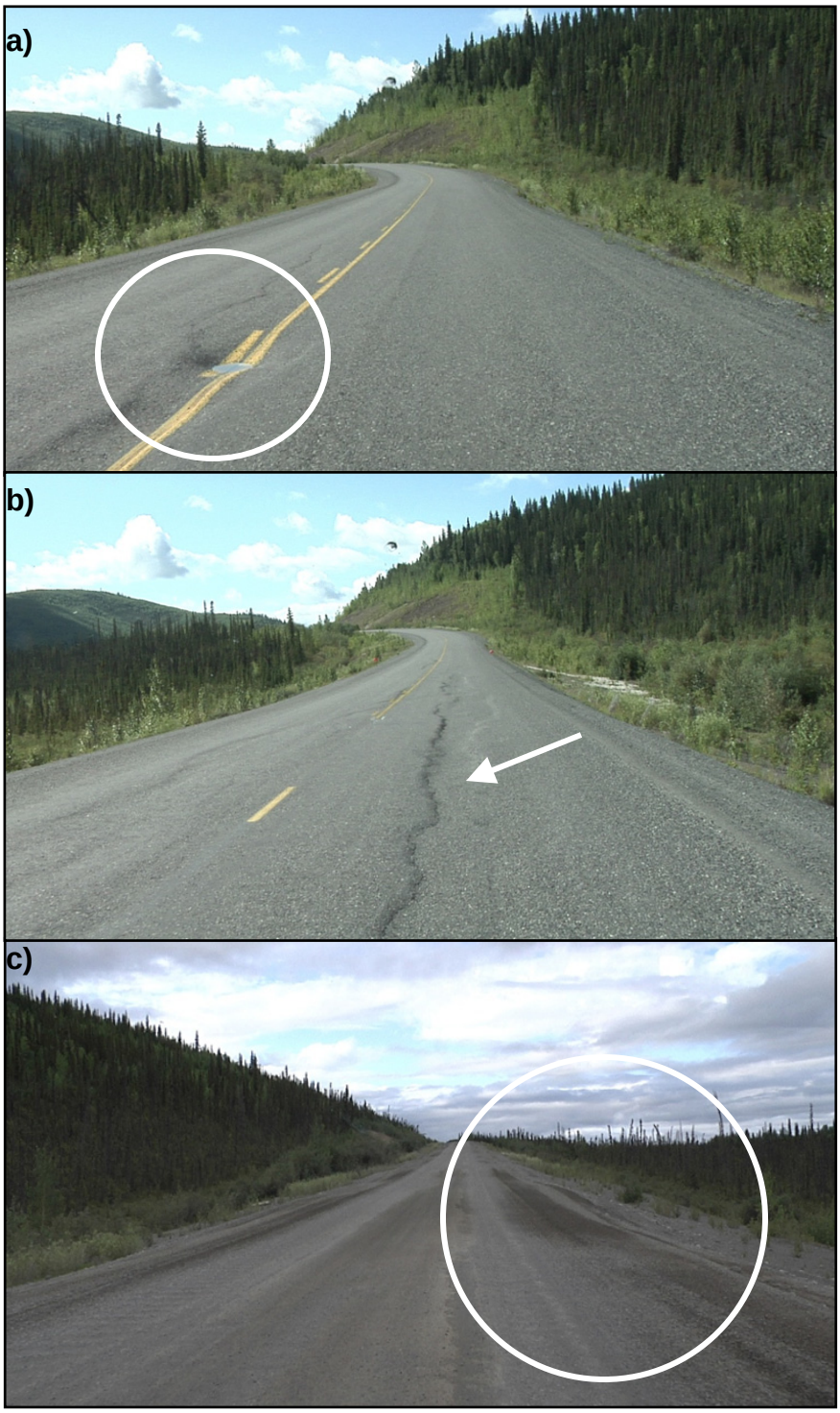


**Figure 6.** Vehicle-level photographs along the Yukon Alaska Highway illustrating a) localized damage (punctual thaw settlement, km 1896.2, 2011), b) linear damage (longitudinal settlement, km 1896.4–1896.2, 2011), and c) general damage (differential settlement of right embankment, km 1894.4–1894.3, 2012).

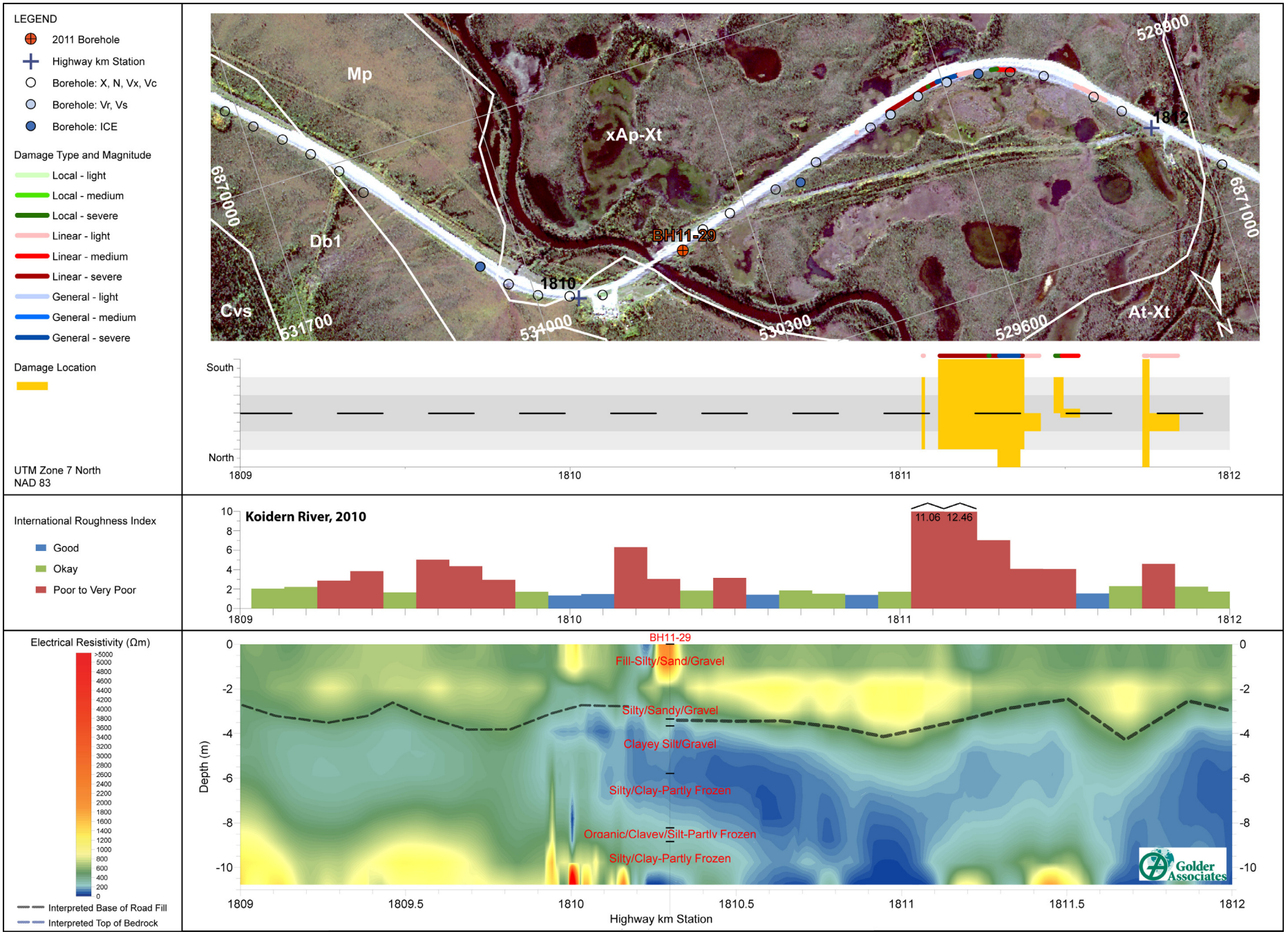


**Figure 7.** Koidern River section, 2010: surficial geology (Lipovsky and Bond, 2014), geotechnical boreholes and ground ice data (Lipovsky, 2009; Lister 2011), damage observations, IRI measurements, and geophysical results (Hammond, 2013).

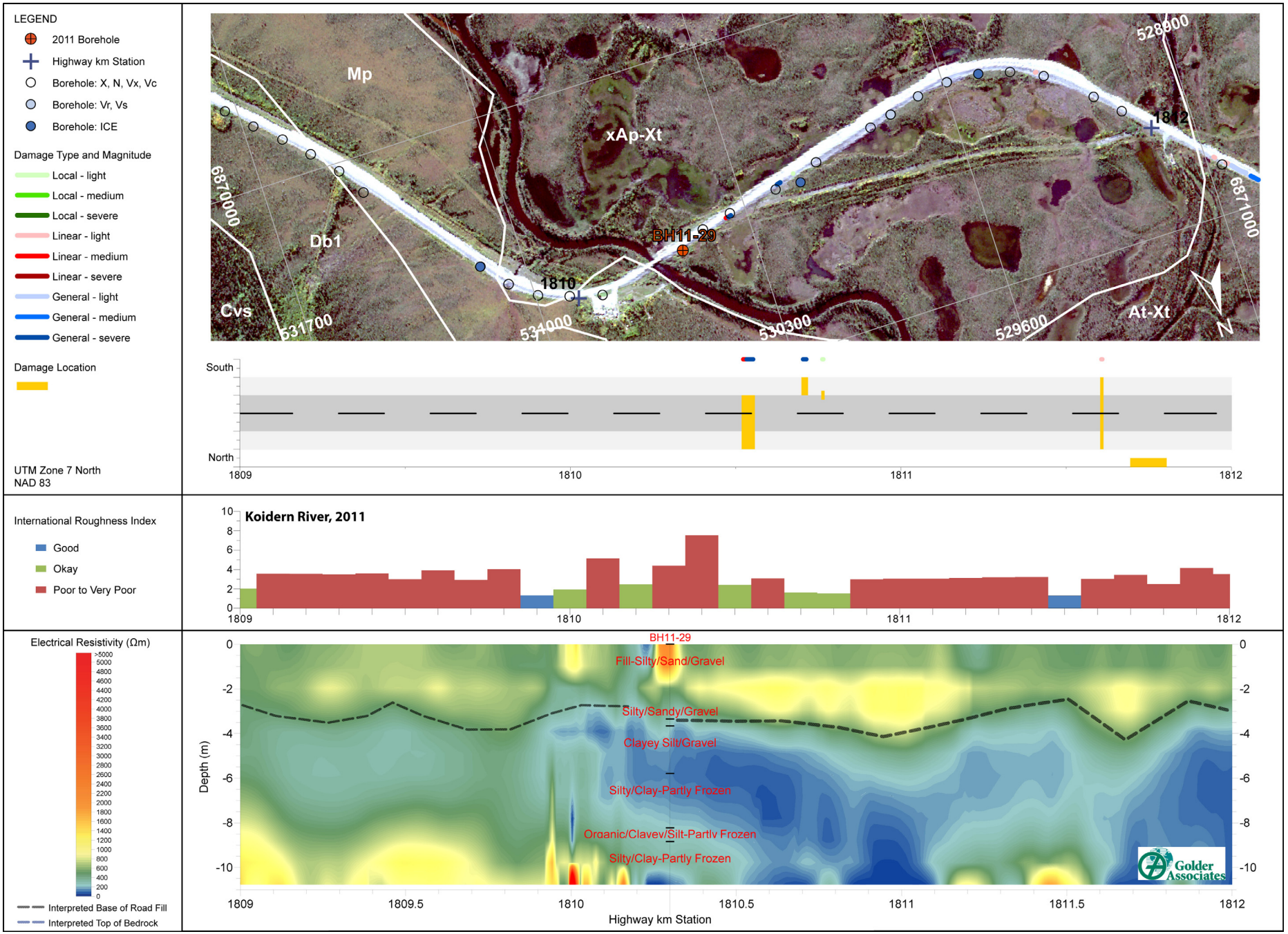


**Figure 8.** Koidern River section, 2011: surficial geology (Lipovsky and Bond, 2014), geotechnical boreholes and ground ice data (Lipovsky, 2009; Lister 2011), damage observations, IRI measurements, and geophysical results (Hammond, 2013).

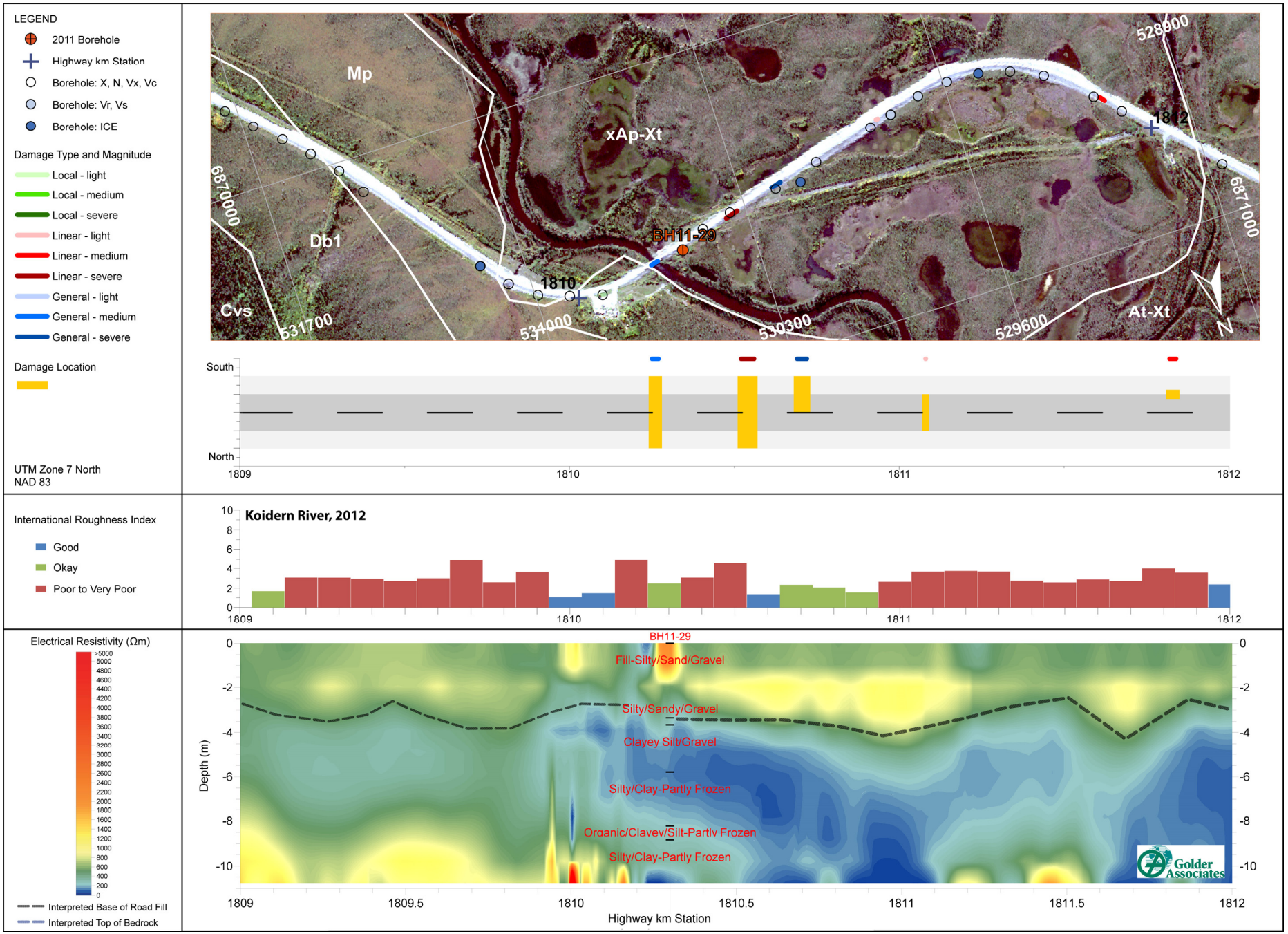


**Figure 9.** Koidern River section, 2012: surficial geology (Lipovsky and Bond, 2014), geotechnical boreholes and ground ice data (Lipovsky, 2009; Lister 2011), damage observations, IRI measurements, and geophysical results (Hammond, 2013).

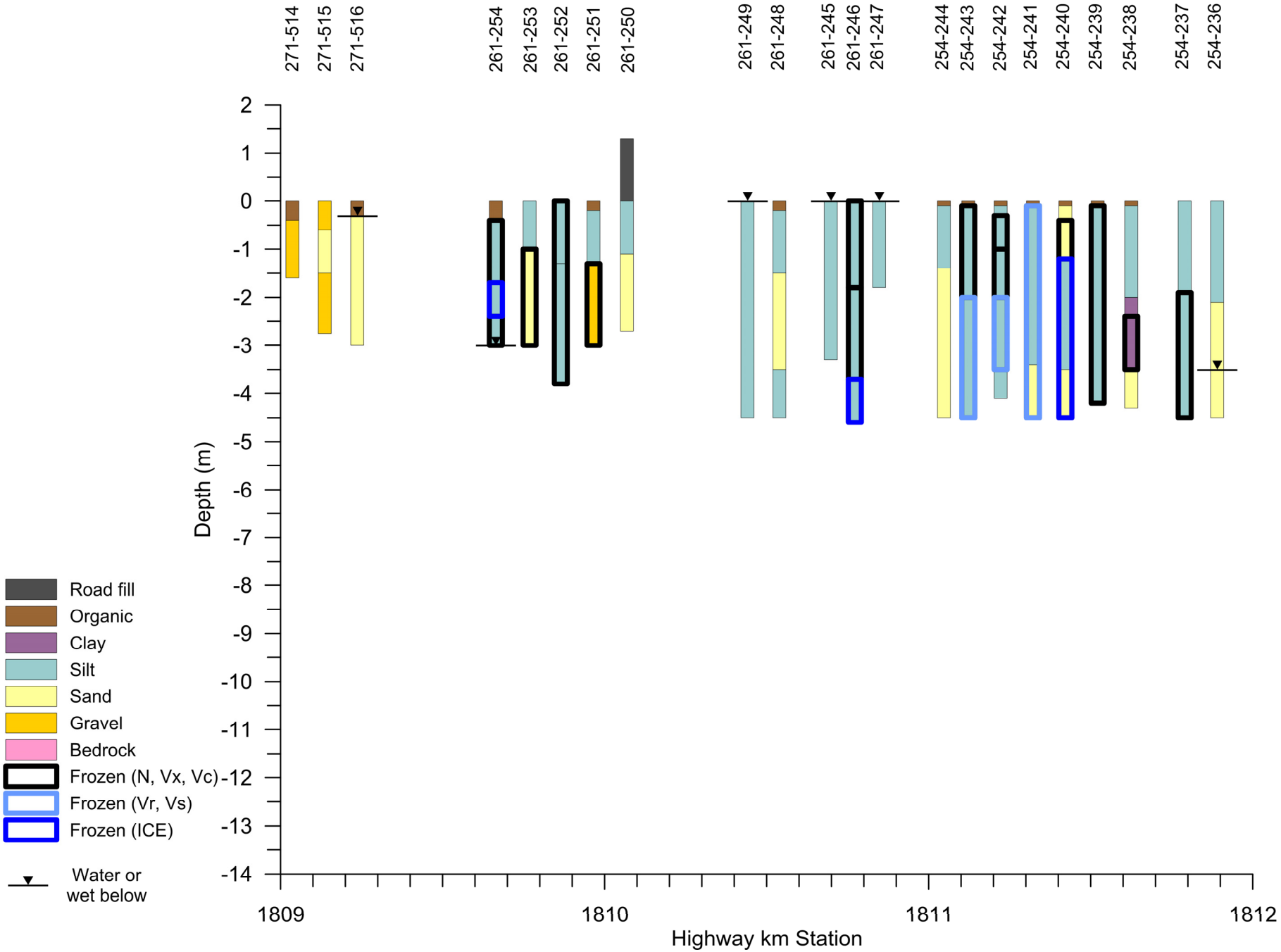


**Figure 10.** Koidern River section: geotechnical sediment texture and ground ice data from boreholes completed in 1993 (Lipovsky, 2009).

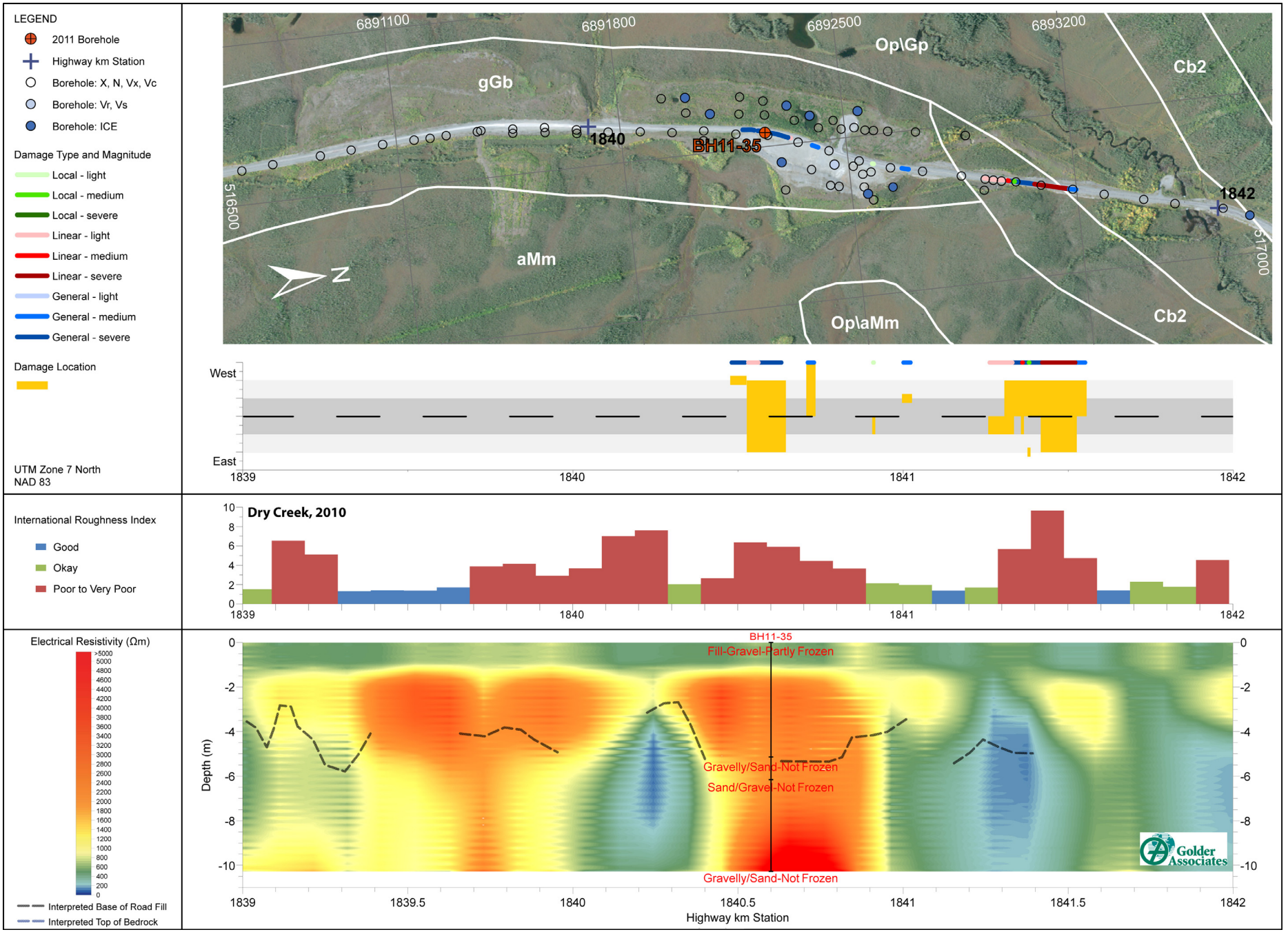


**Figure 11.** Dry Creek section, 2010: surficial geology (Lipovsky and Bond, 2014), geotechnical boreholes and ground ice data (Lipovsky, 2009; Lister 2011), damage observations, IRI measurements, and geophysical results (Hammond, 2013).

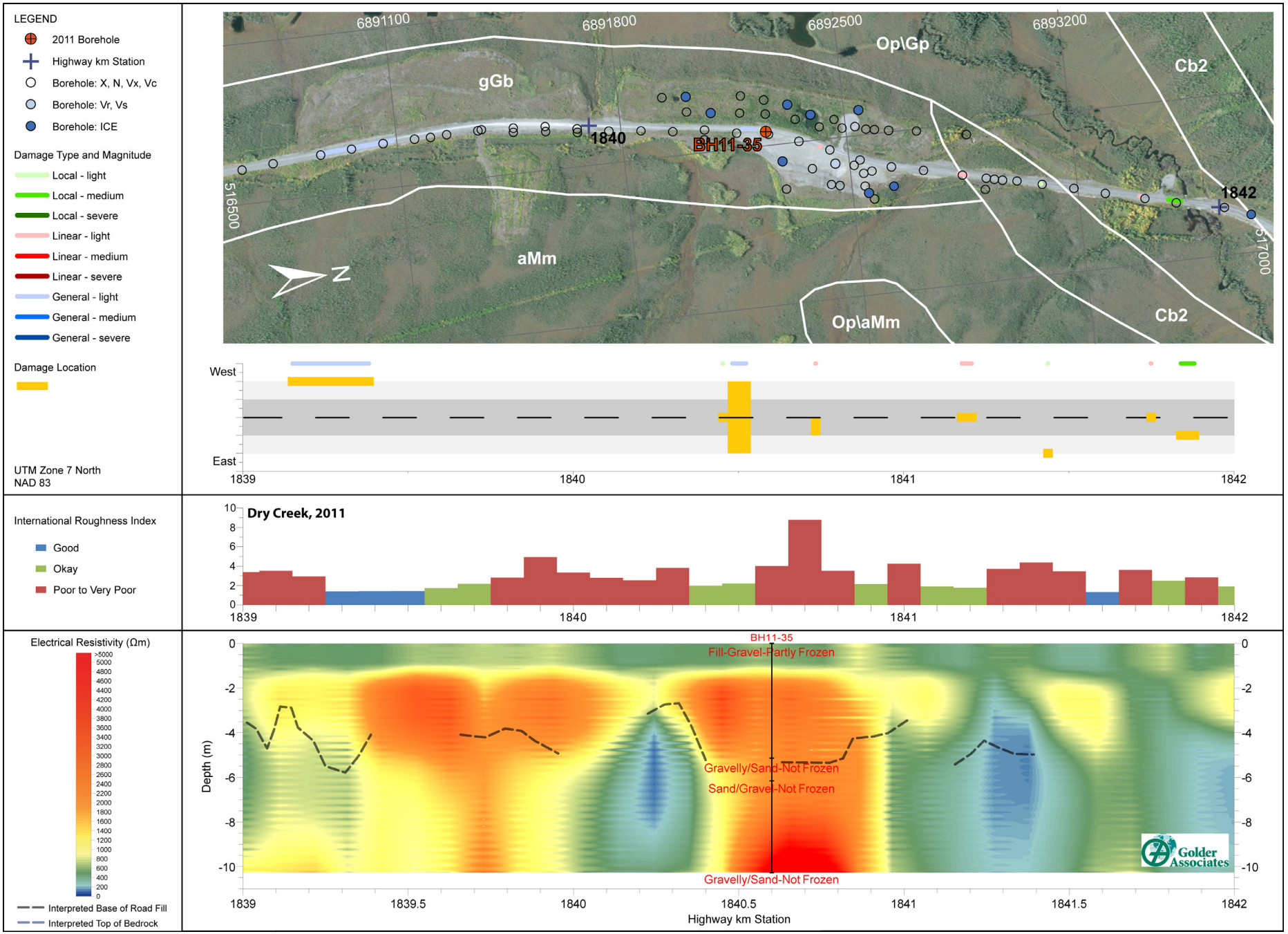


**Figure 12.** Dry Creek section, 2011: surficial geology (Lipovsky and Bond, 2014), geotechnical boreholes and ground ice data (Lipovsky, 2009; Lister 2011), damage observations, IRI measurements, and geophysical results (Hammond, 2013).

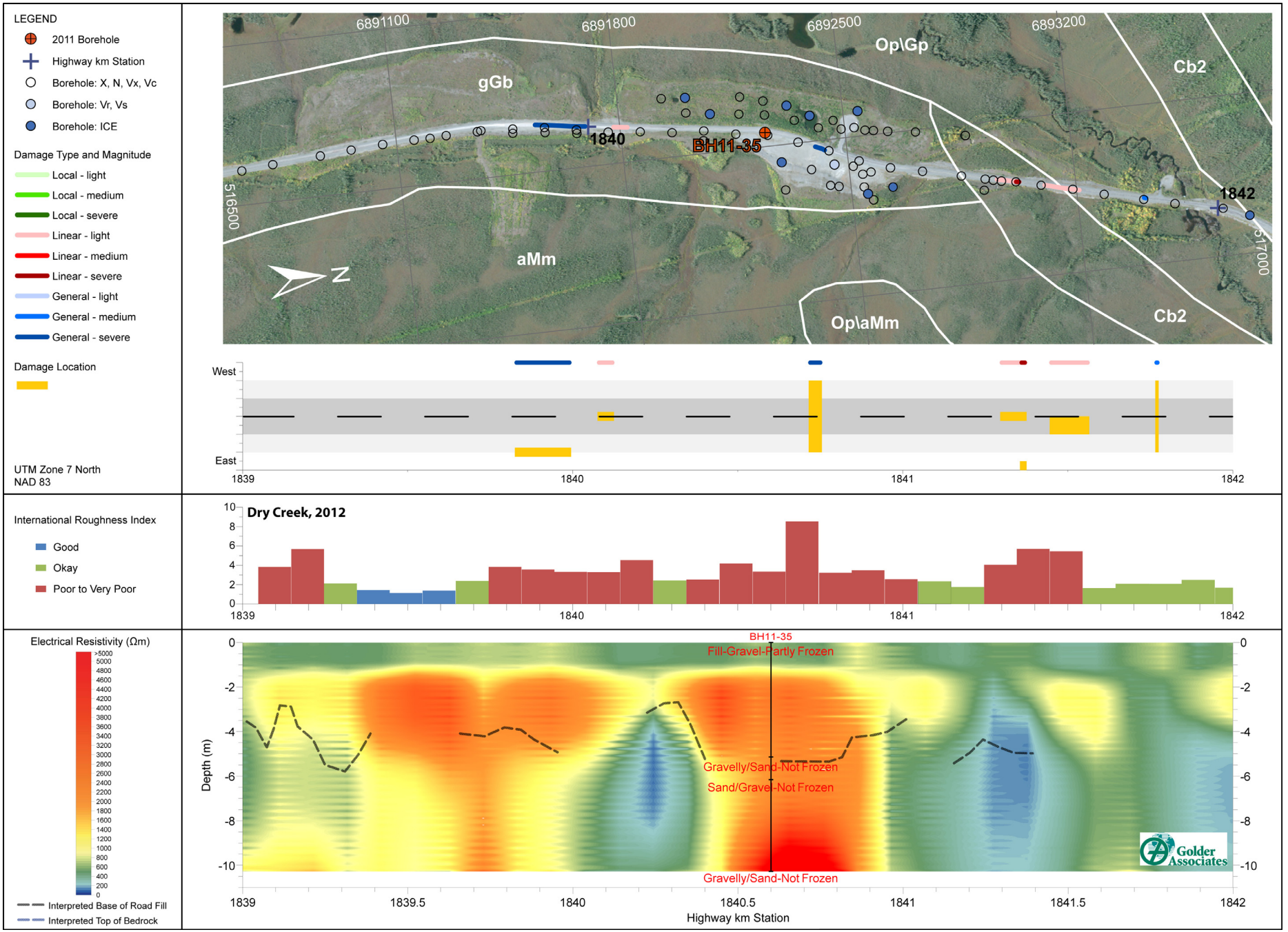


**Figure 13.** Dry Creek section, 2012: surficial geology (Lipovsky and Bond, 2014), geotechnical boreholes and ground ice data (Lipovsky, 2009; Lister 2011), damage observations, IRI measurements, and geophysical results (Hammond, 2013).

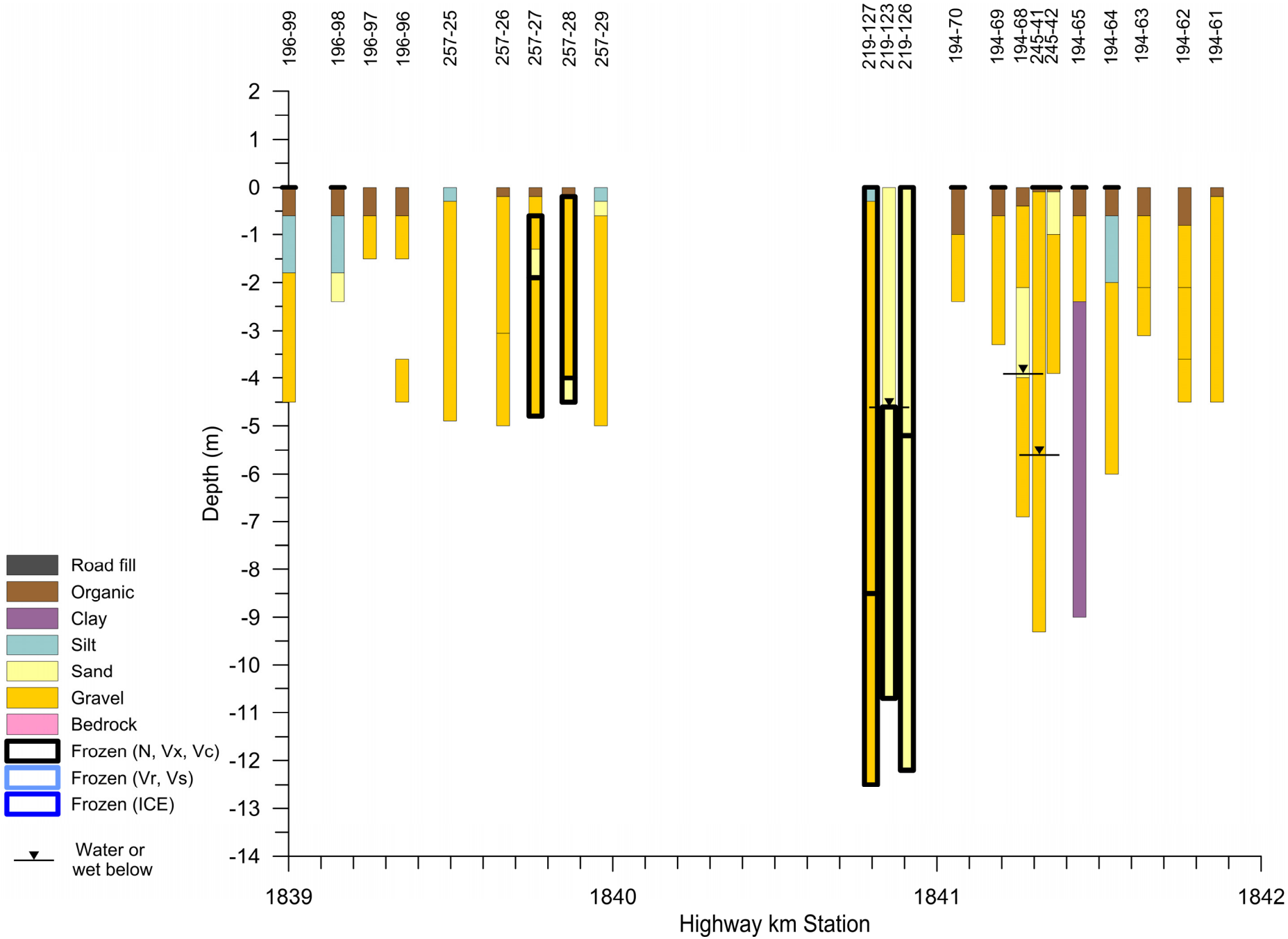


**Figure 14.** Dry Creek section: geotechnical sediment texture and ground ice data from boreholes completed in 1992–1994 (Lipovsky, 2009). Select boreholes located along the road. On-road boreholes from 1840–1840.7 have no geotechnical data.

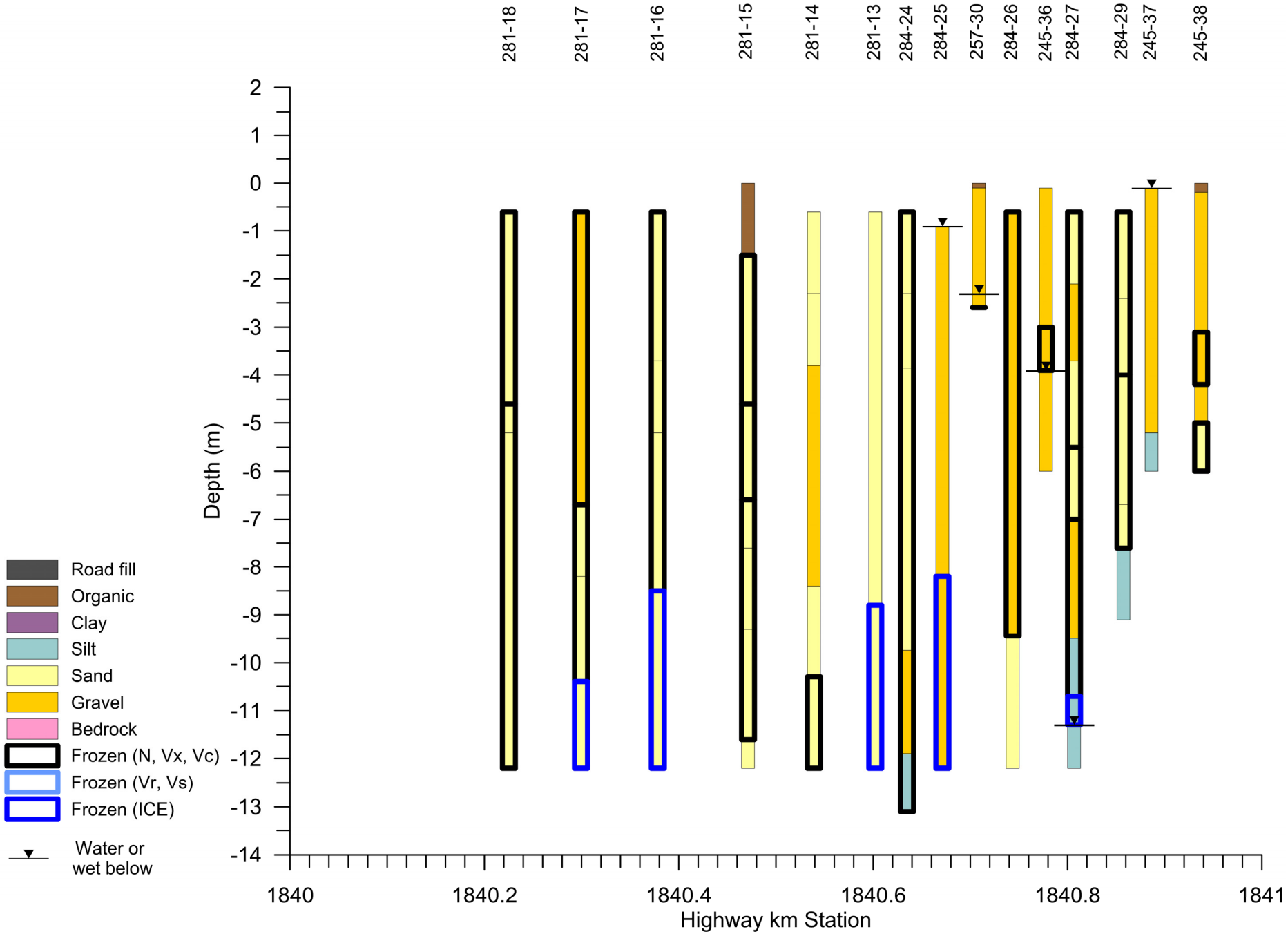


**Figure 15.** Dry Creek section: geotechnical sediment texture and ground ice data from boreholes completed in 1992–1994 (Lipovsky, 2009). Select boreholes located west of the road.

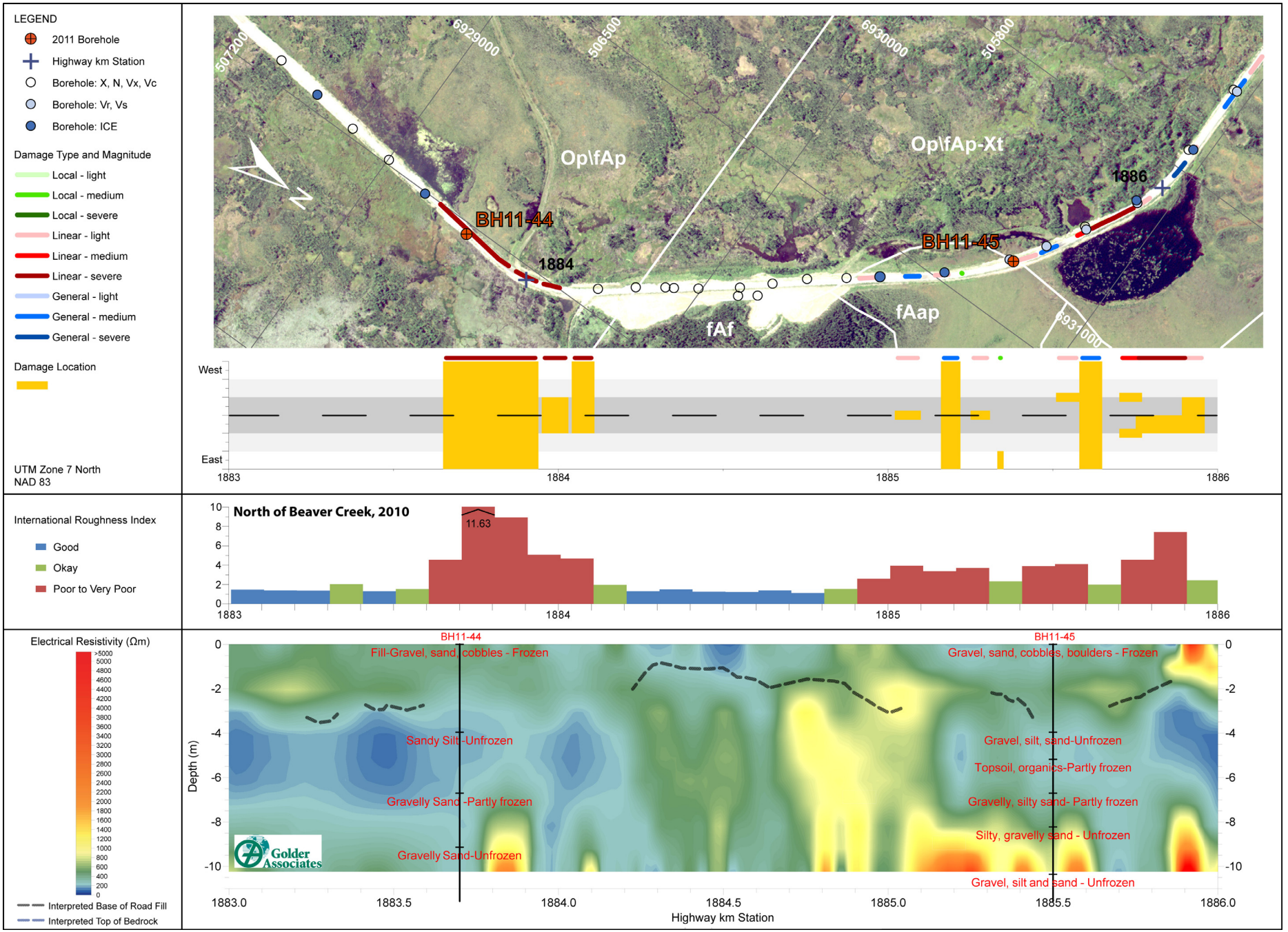


**Figure 16.** North of Beaver Creek section, part 1, 2010: surficial geology (Lipovsky and Bond, 2014), geotechnical boreholes and ground ice data (Lipovsky, 2009; Lister 2011), damage observations, IRI measurements, and geophysical results (Hammond, 2013).

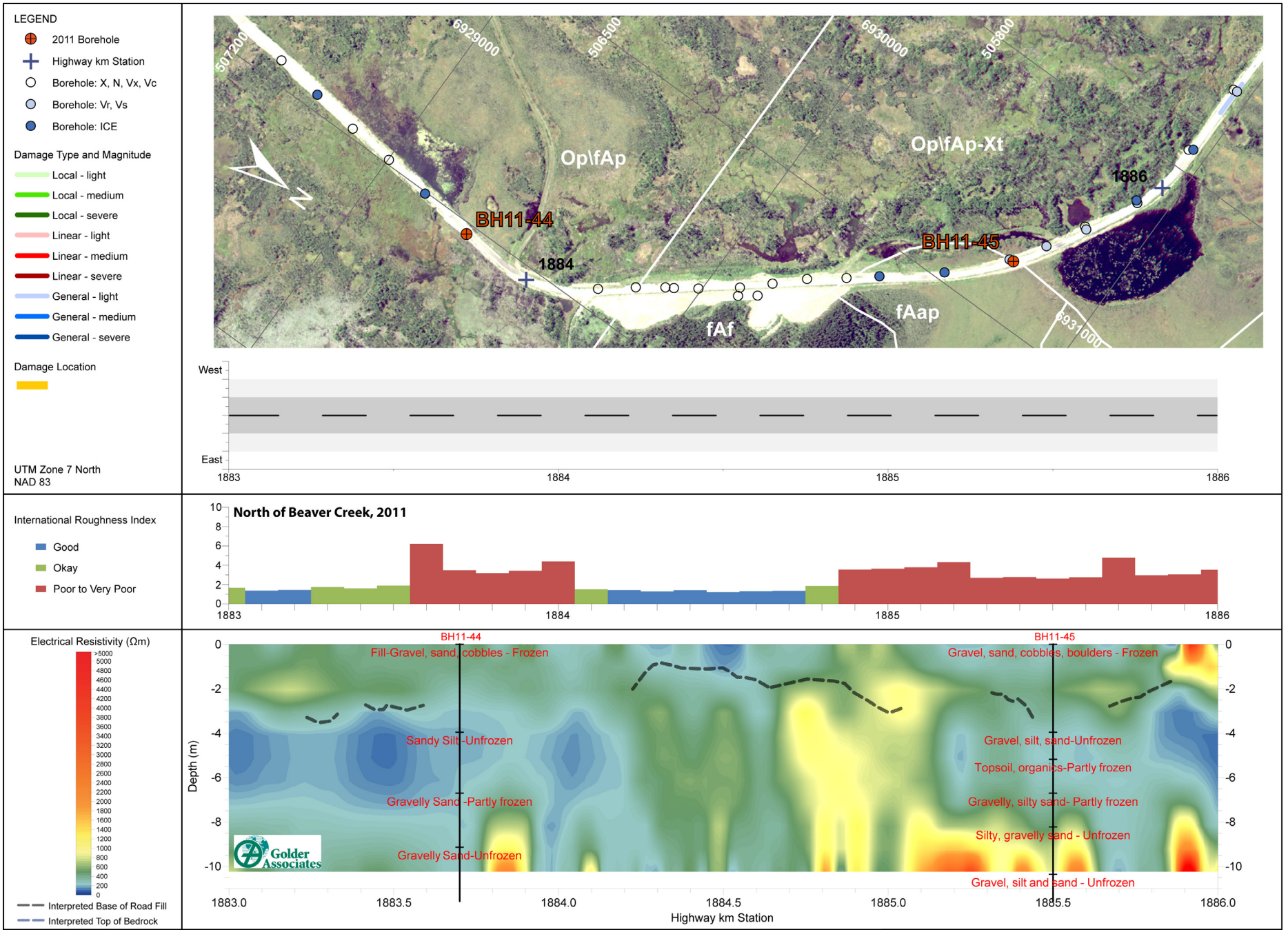


**Figure 17.** North of Beaver Creek section, part 1, 2011: surficial geology (Lipovsky and Bond, 2014), geotechnical boreholes and ground ice data (Lipovsky, 2009; Lister 2011), damage observations, IRI measurements, and geophysical results (Hammond, 2013).

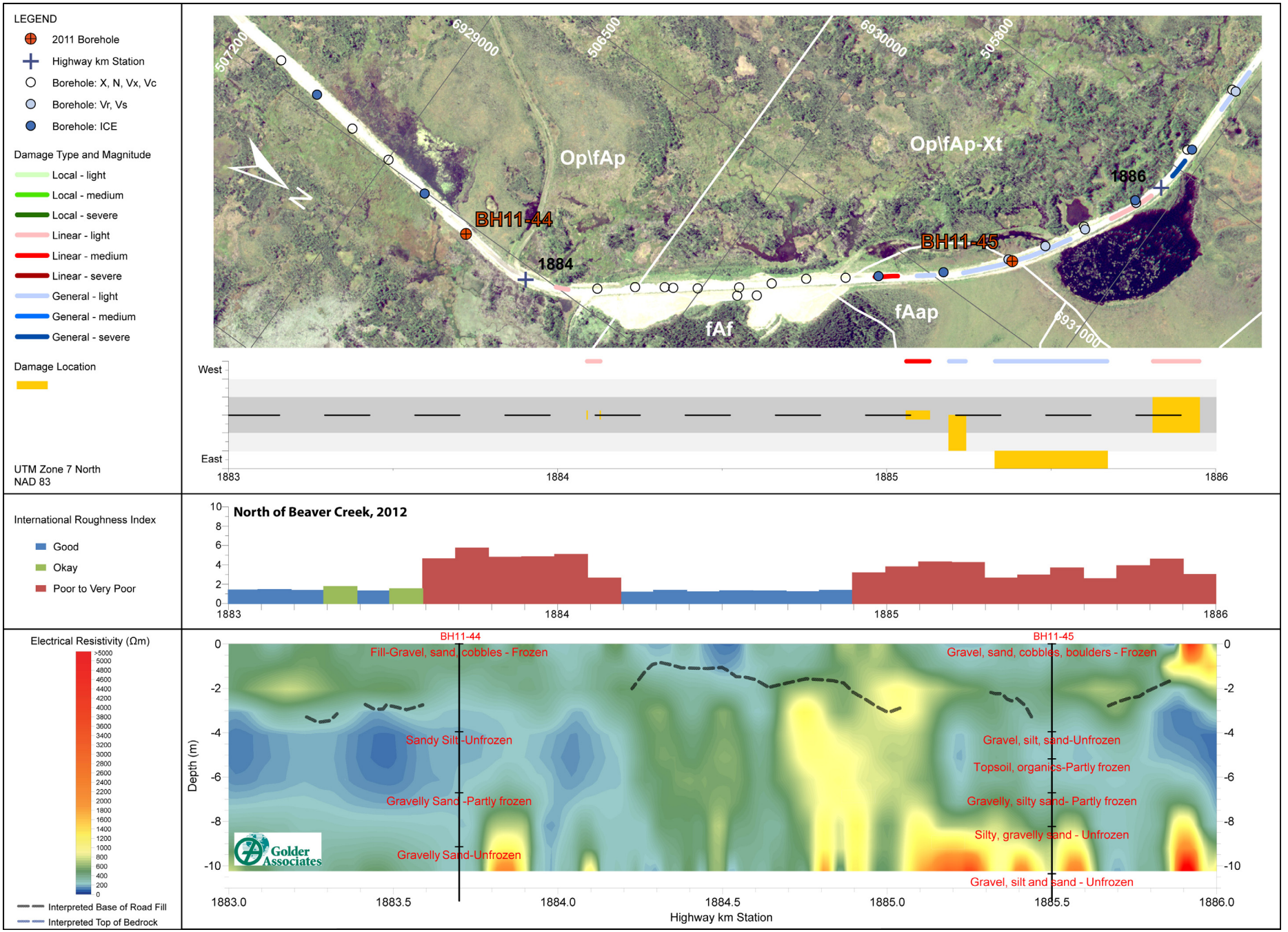


**Figure 18.** North of Beaver Creek section, part 1, 2012: surficial geology (Lipovsky and Bond, 2014), geotechnical boreholes and ground ice data (Lipovsky, 2009; Lister 2011), damage observations, IRI measurements, and geophysical results (Hammond, 2013).

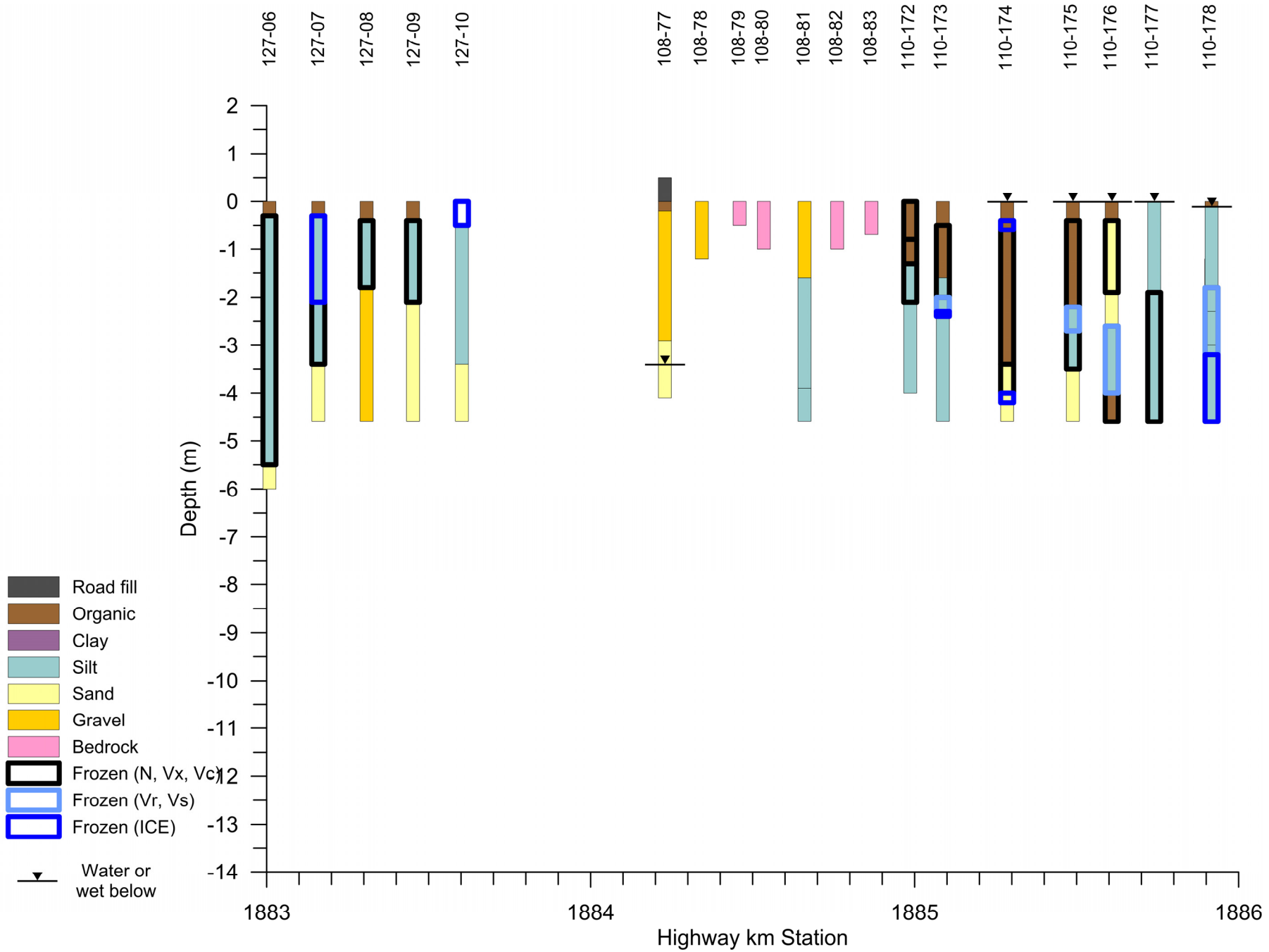


**Figure 19.** North of Beaver Creek section, part 1: geotechnical borehole lithology and ground ice data from boreholes completed in 1990–1991 (Lipovsky, 2009). Select boreholes.

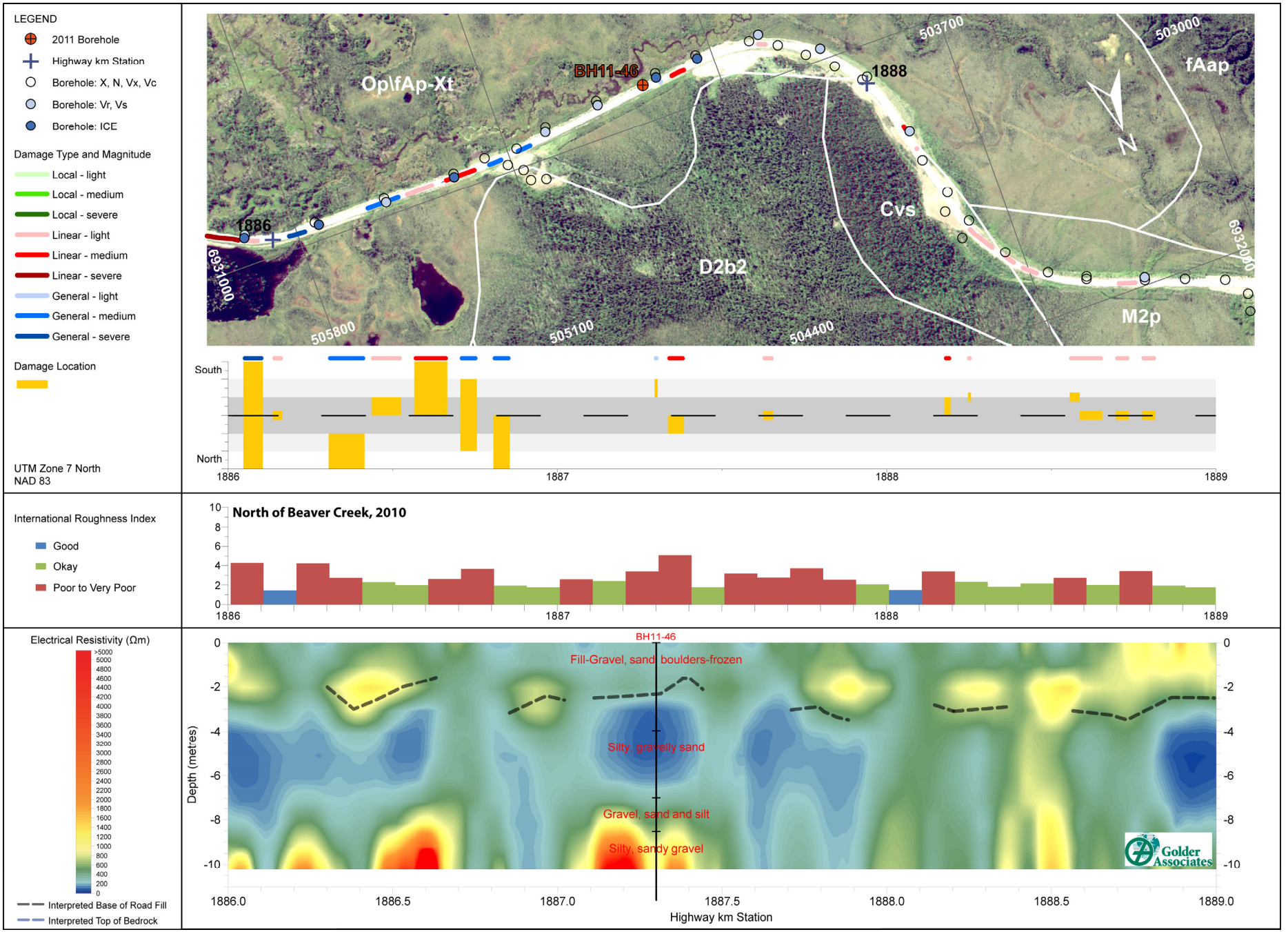


**Figure 20.** North of Beaver Creek section, part 2, 2010: surficial geology (Lipovsky and Bond, 2014), geotechnical boreholes and ground ice data (Lipovsky, 2009; Lister 2011), damage observations, IRI measurements, and geophysical results (Hammond, 2013).

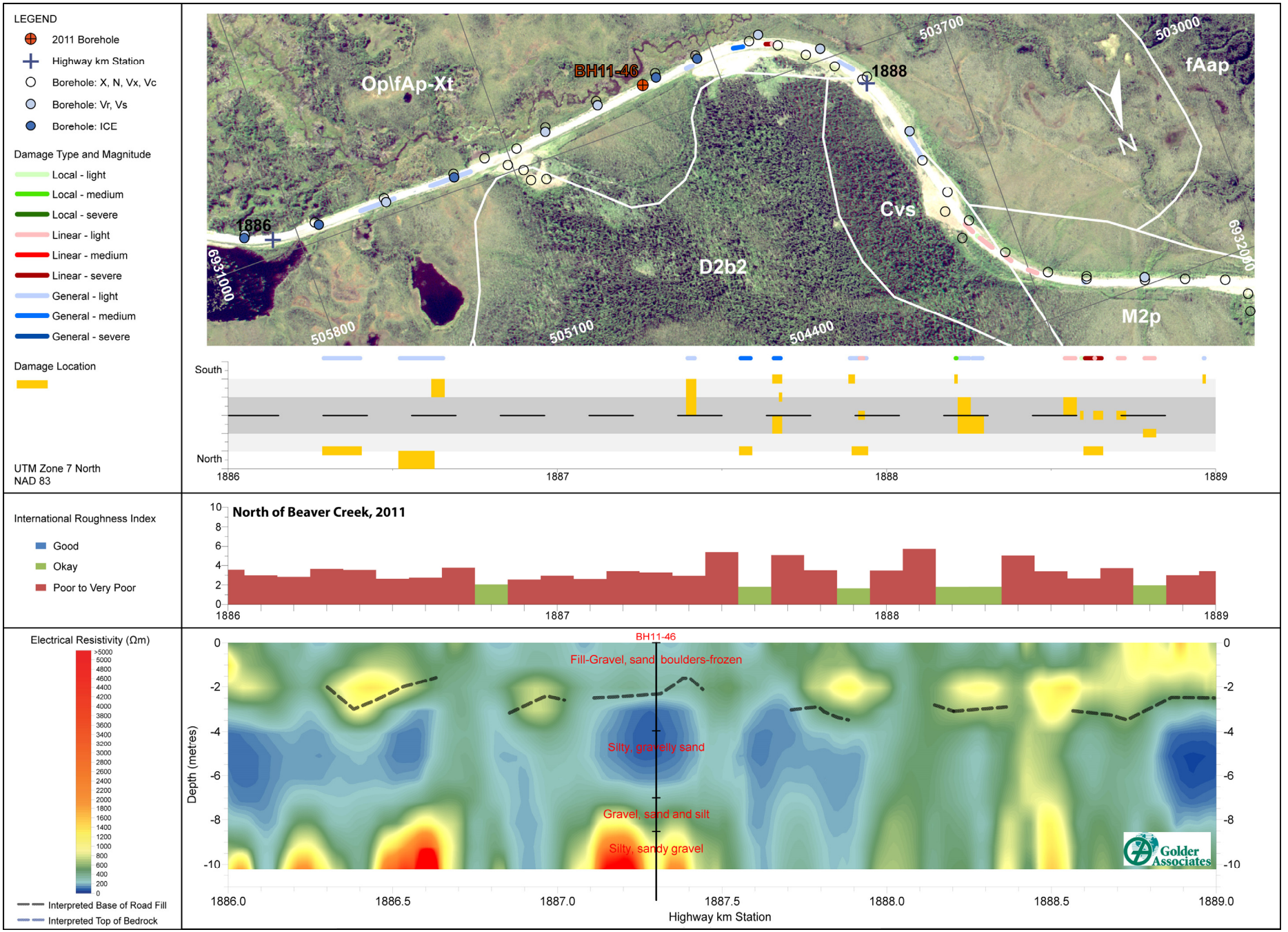


**Figure 21.** North of Beaver Creek section, part 2, 2011: surficial geology (Lipovsky and Bond, 2014), geotechnical boreholes and ground ice data (Lipovsky, 2009; Lister 2011), damage observations, IRI measurements, and geophysical results (Hammond, 2013).

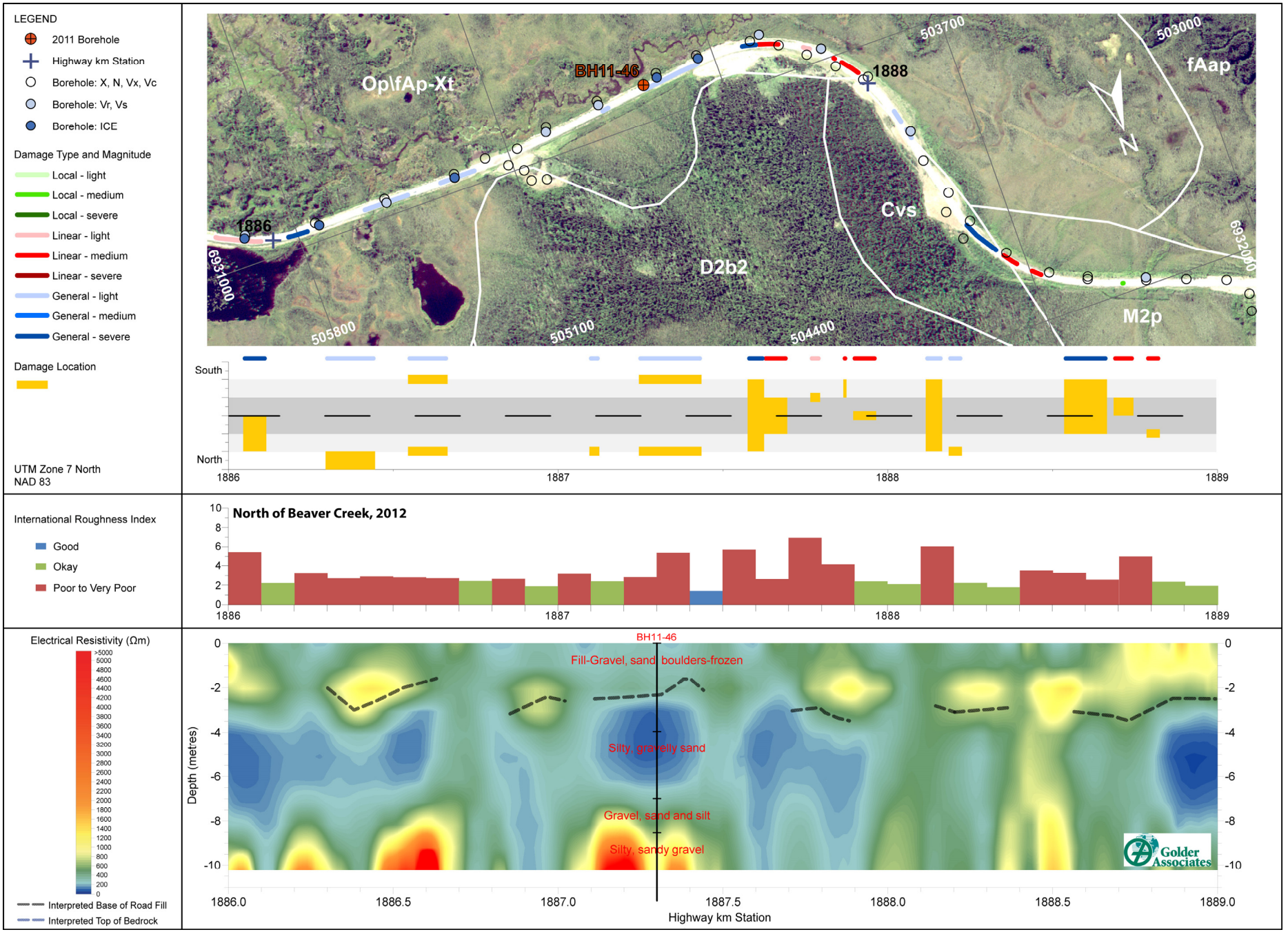


**Figure 22.** North of Beaver Creek section, part 2, 2012: surficial geology (Lipovsky and Bond, 2014), geotechnical boreholes and ground ice data (Lipovsky, 2009; Lister 2011), damage observations, IRI measurements, and geophysical results (Hammond, 2013).

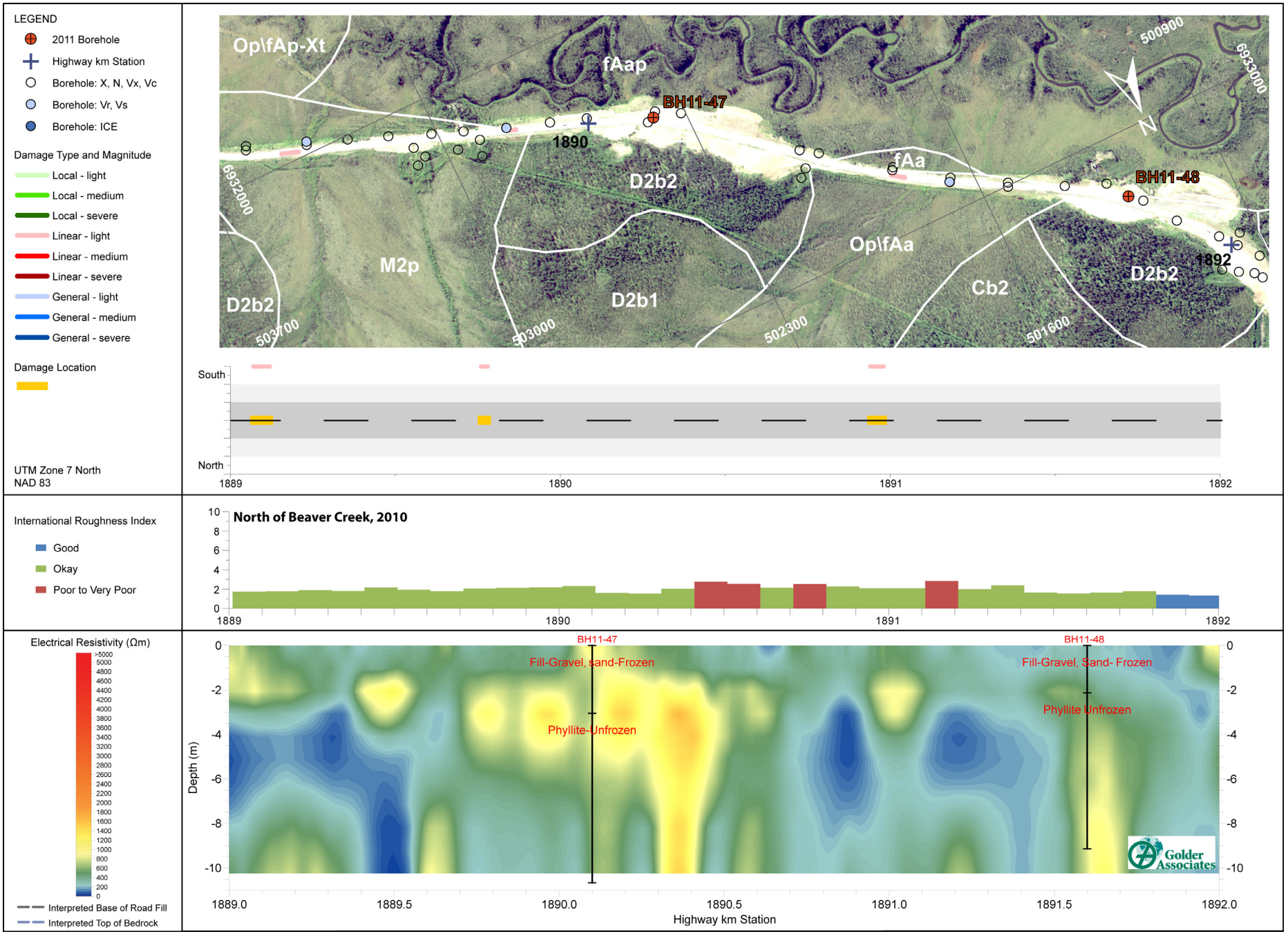


**Figure 23.** North of Beaver Creek section, part 3, 2010: surficial geology (Lipovsky and Bond, 2014), geotechnical boreholes and ground ice data (Lipovsky, 2009; Lister 2011), damage observations, IRI measurements, and geophysical results (Hammond, 2013).

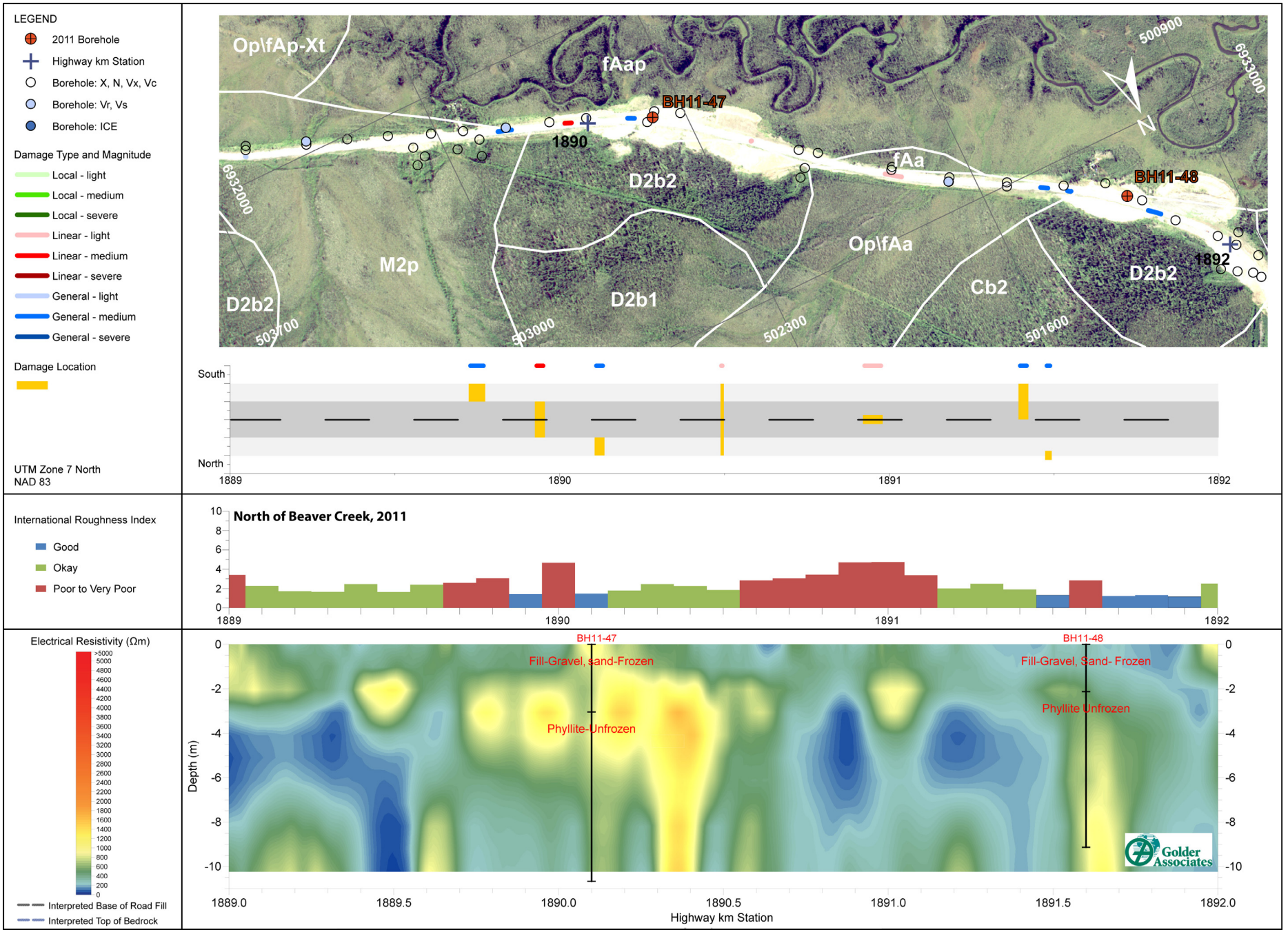


**Figure 24.** North of Beaver Creek section, part 3, 2011: surficial geology (Lipovsky and Bond, 2014), geotechnical boreholes and ground ice data (Lipovsky, 2009; Lister 2011), damage observations, IRI measurements, and geophysical results (Hammond, 2013).

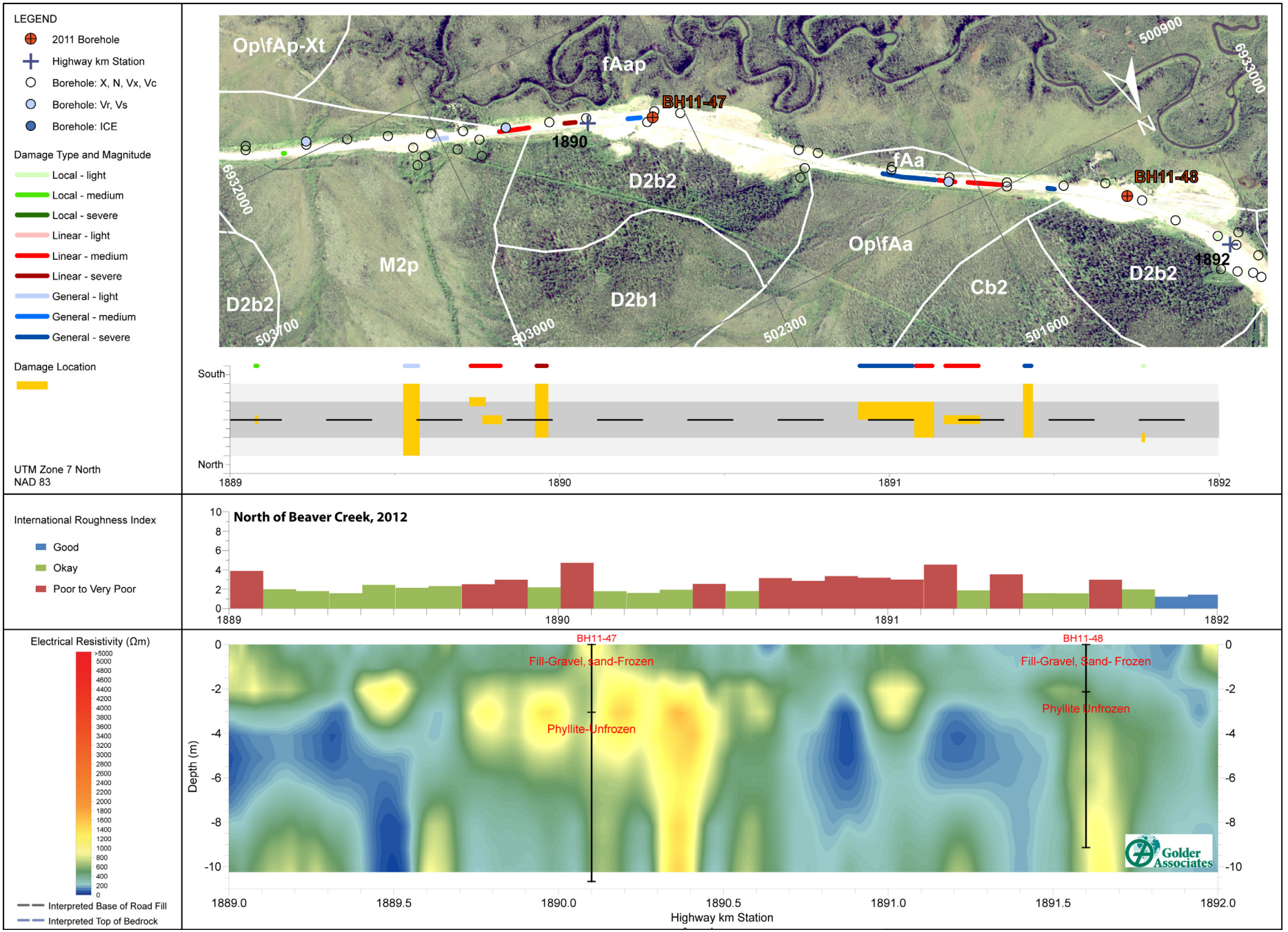


**Figure 25.** North of Beaver Creek section, part 3, 2012: surficial geology (Lipovsky and Bond, 2014), geotechnical boreholes and ground ice data (Lipovsky, 2009; Lister 2011), damage observations, IRI measurements, and geophysical results (Hammond, 2013).

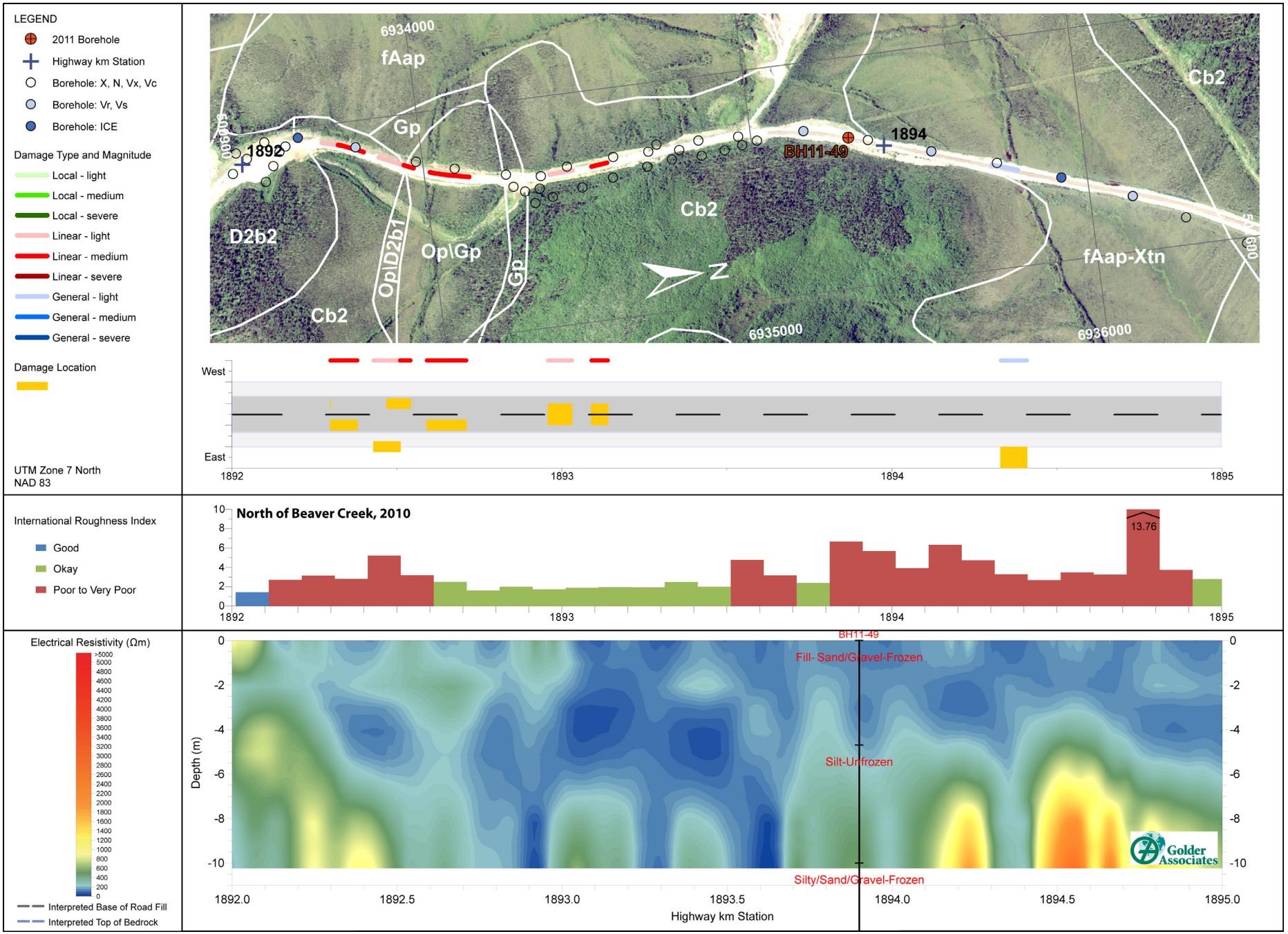


**Figure 26.** North of Beaver Creek section, part 4, 2010: surficial geology (Lipovsky and Bond, 2014), geotechnical boreholes and ground ice data (Lipovsky, 2009; Lister 2011), damage observations, IRI measurements, and geophysical results (Hammond, 2013).

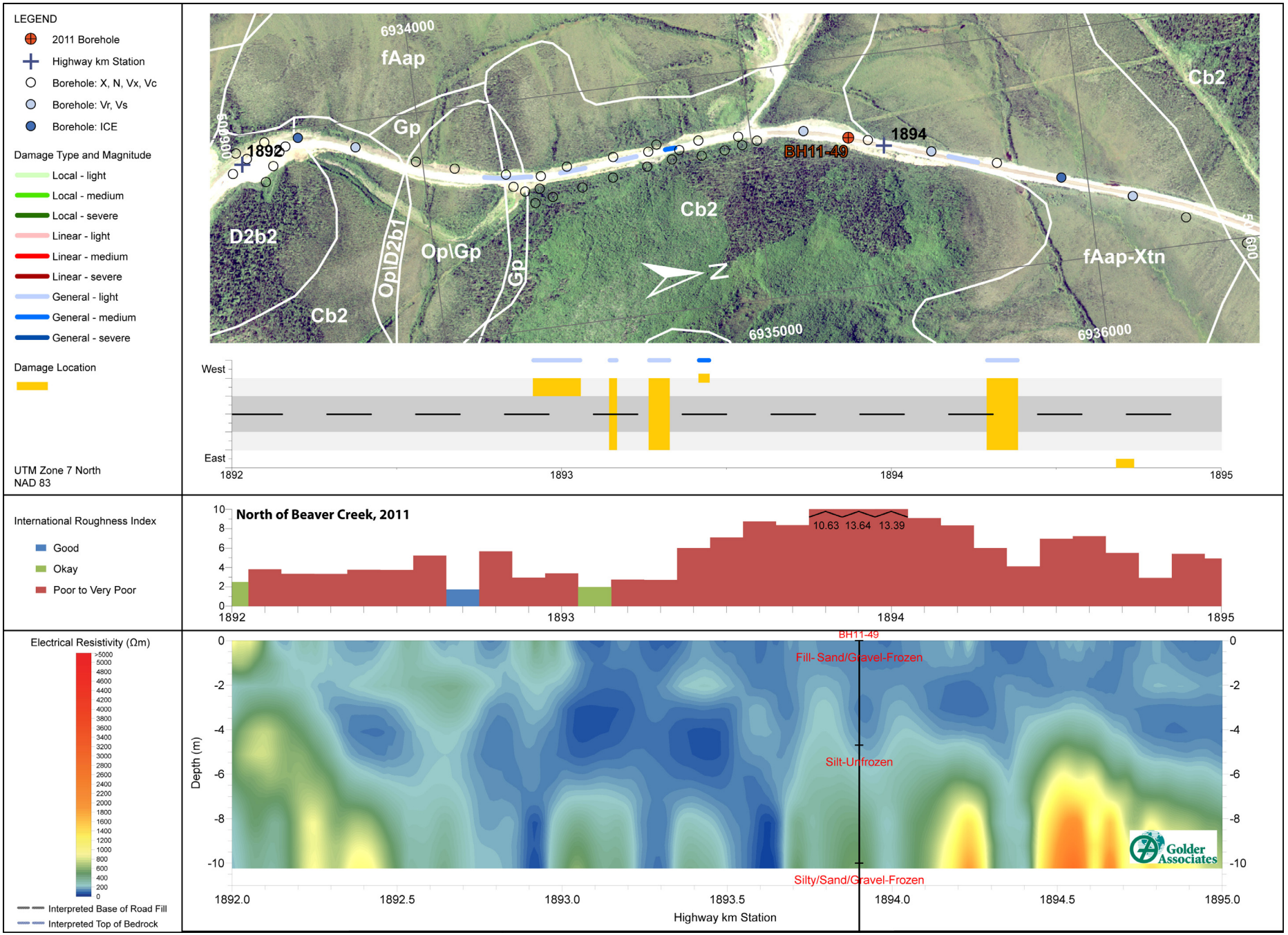


**Figure 27.** North of Beaver Creek section, part 4, 2011: surficial geology (Lipovsky and Bond, 2014), geotechnical boreholes and ground ice data (Lipovsky, 2009; Lister 2011), damage observations, IRI measurements, and geophysical results (Hammond, 2013).

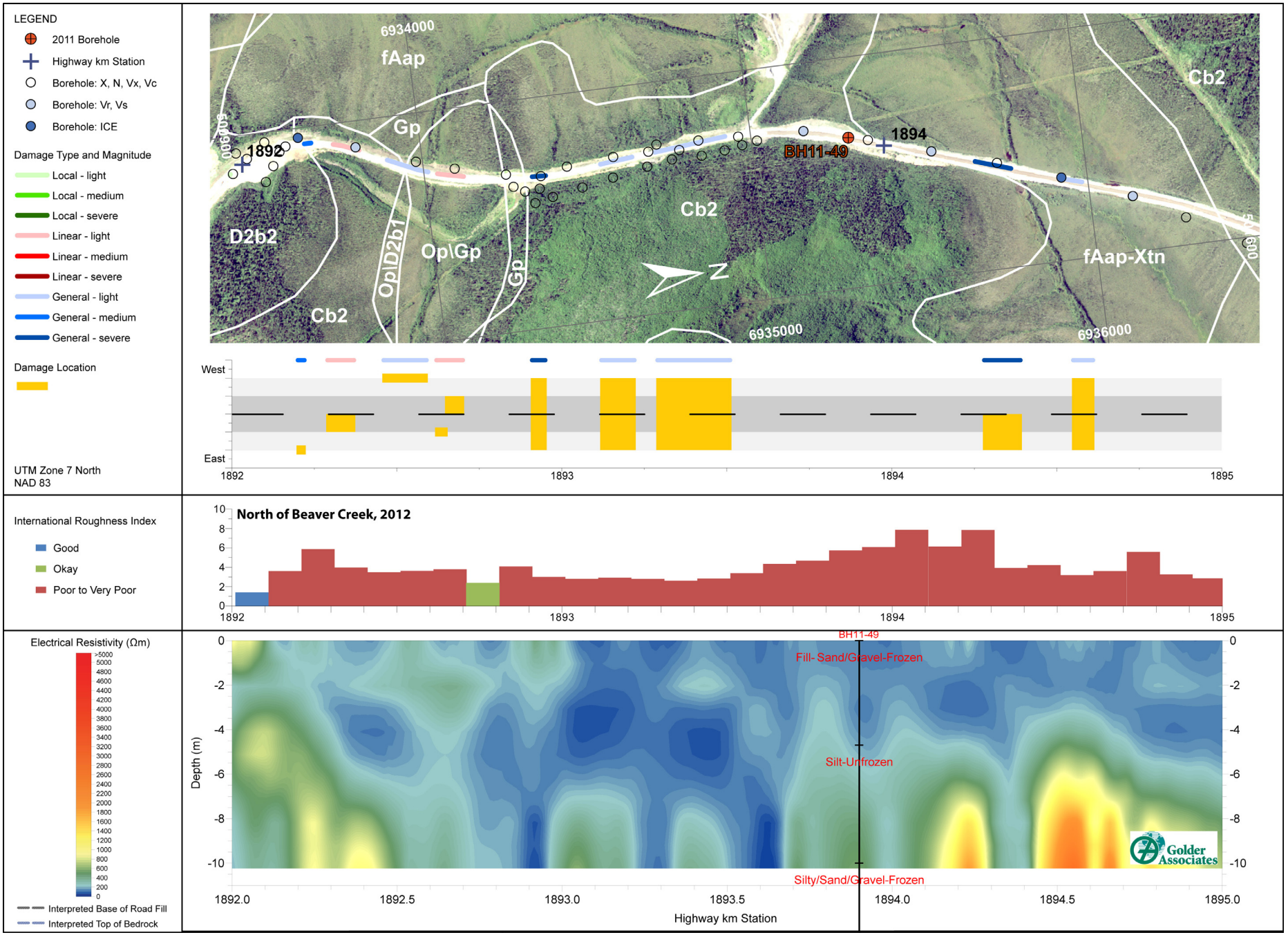


**Figure 28.** North of Beaver Creek section, part 4, 2012: surficial geology (Lipovsky and Bond, 2014), geotechnical boreholes and ground ice data (Lipovsky, 2009; Lister 2011), damage observations, IRI measurements, and geophysical results (Hammond, 2013).

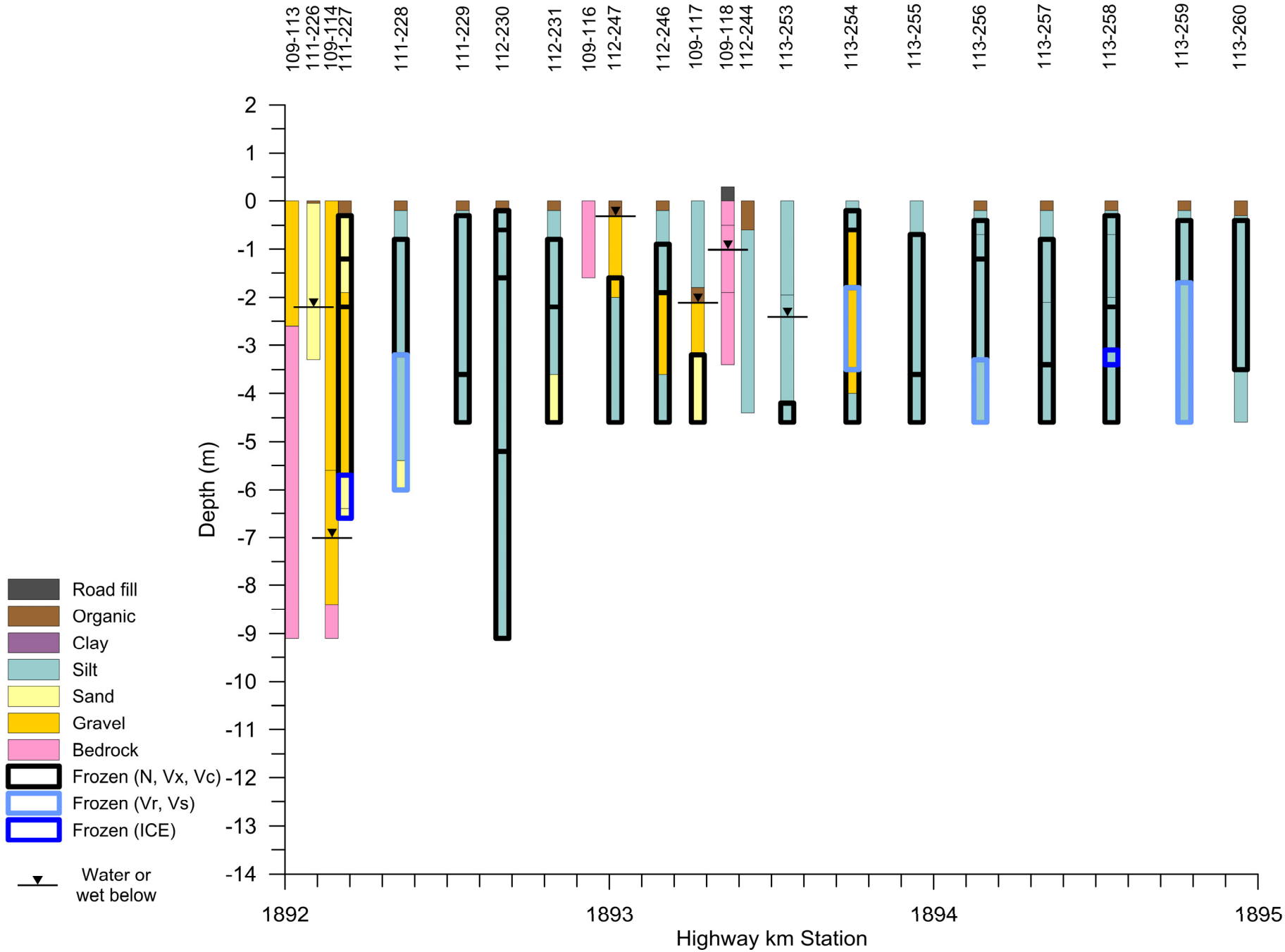


**Figure 29.** North of Beaver Creek section, part 4: geotechnical sediment texture and ground ice data from boreholes completed in 1990 (Lipovsky, 2009). Select boreholes.

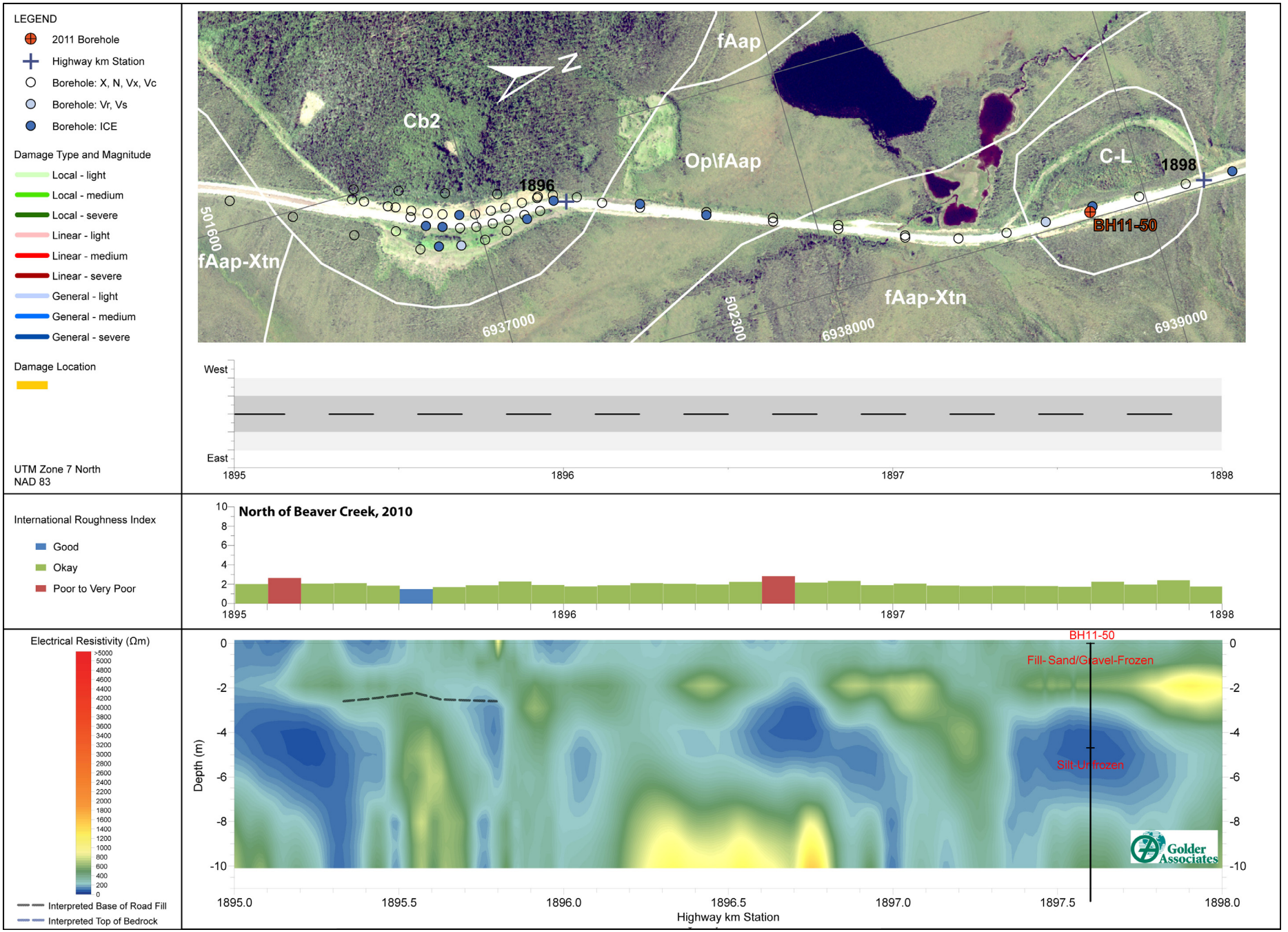


**Figure 30.** North of Beaver Creek section, part 5, 2010: surficial geology (Lipovsky and Bond, 2014), geotechnical boreholes and ground ice data (Lipovsky, 2009; Lister 2011), damage observations, IRI measurements, and geophysical results (Hammond, 2013).

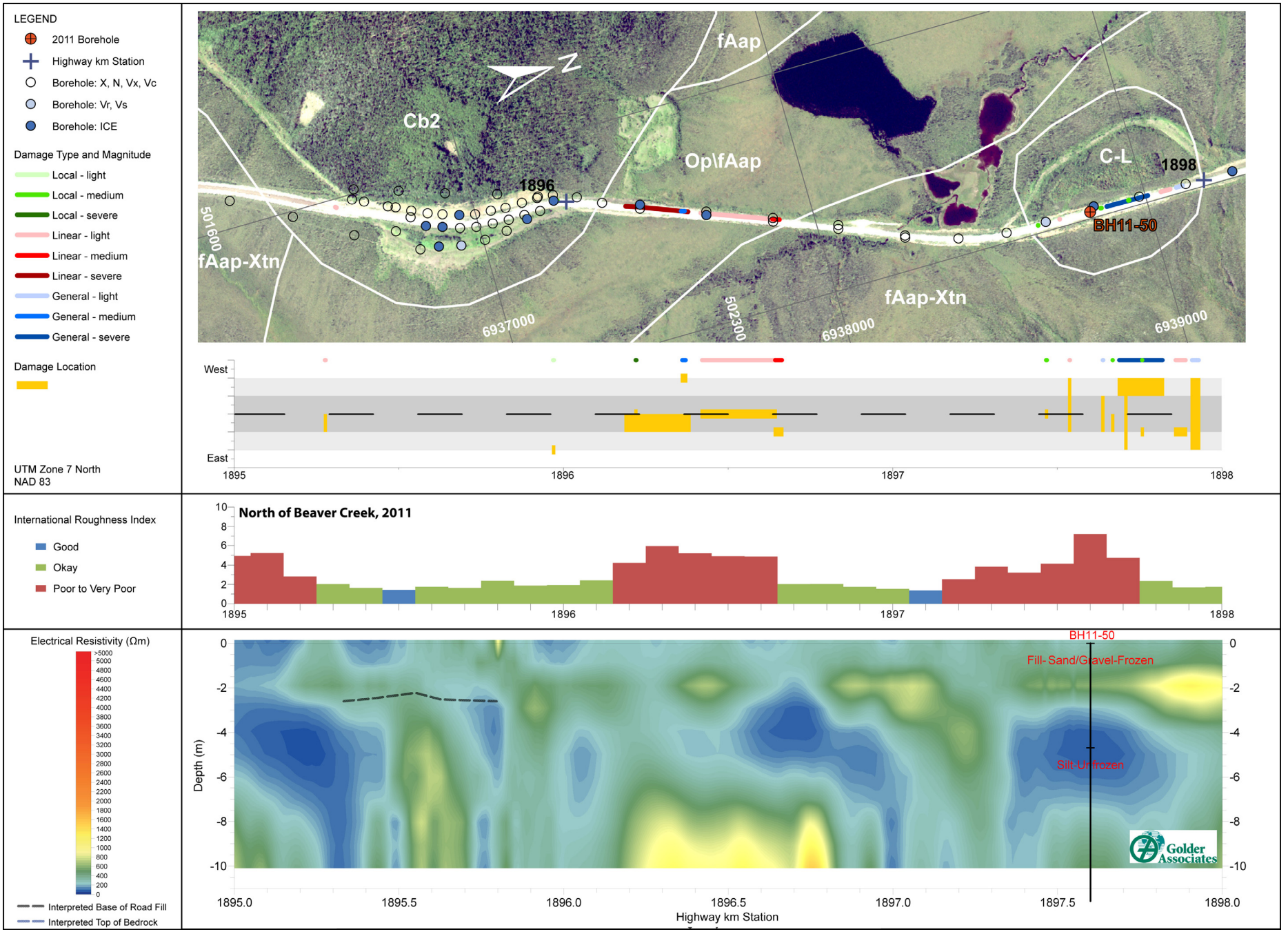


**Figure 31.** North of Beaver Creek section, part 5, 2011: surficial geology (Lipovsky and Bond, 2014), geotechnical boreholes and ground ice data (Lipovsky, 2009; Lister 2011), damage observations, IRI measurements, and geophysical results (Hammond, 2013).

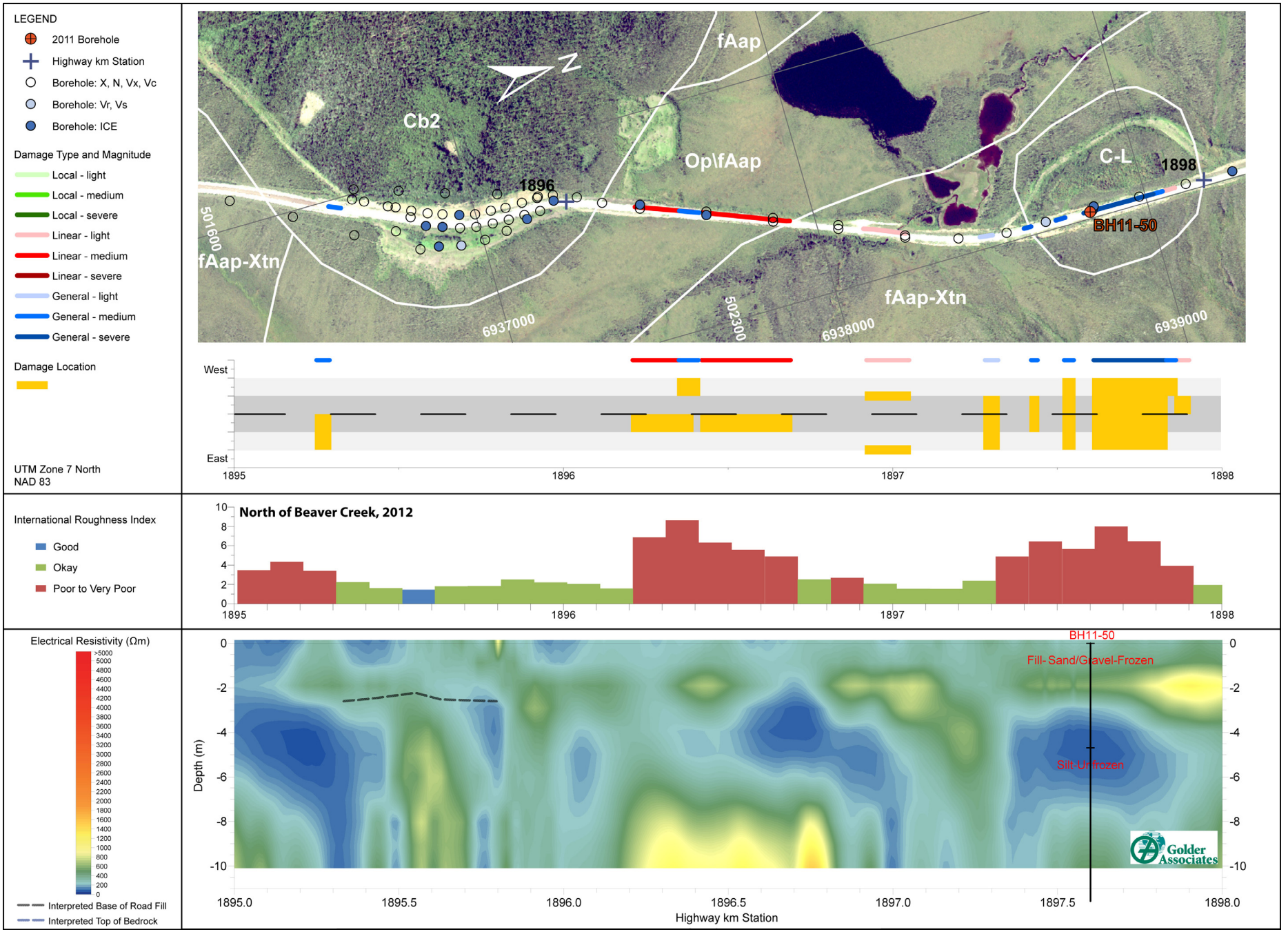


**Figure 32.** North of Beaver Creek section, part 5, 2012: surficial geology (Lipovsky and Bond, 2014), geotechnical boreholes and ground ice data (Lipovsky, 2009; Lister 2011), damage observations, IRI measurements, and geophysical results (Hammond, 2013).

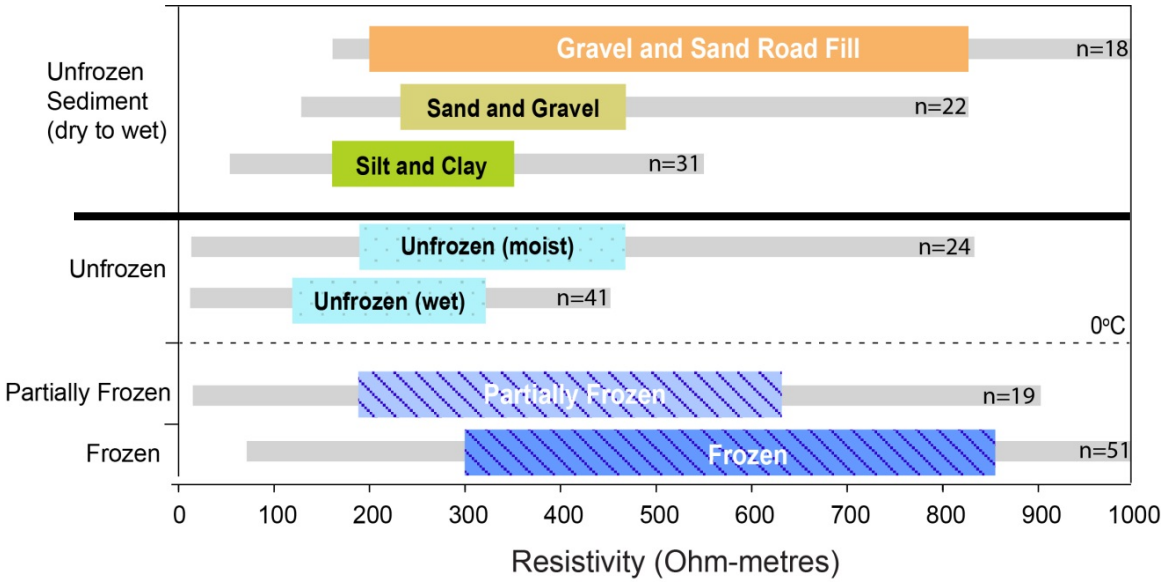


**Figure 33.** Electrical resistivity ranges observed for unfrozen sediment type, moist and wet unfrozen sediment, and partially frozen and frozen sediment at 20 selected geotechnical borehole locations from 2011 and 2013 (bold font in Figure 2; Stevens, 2014). Grey bars indicate the range between minimum and maximum resistivity and the coloured boxes indicate the range between the 25th and 75th percentiles.